# TRACING THE ECOPHYSIOLOGY OF UNGULATES AND PREDATOR-PREY RELATIONSHIPS IN AN EARLY PLEISTOCENE LARGE MAMMAL COMMUNITY

Paul Palmqvist [a,*], Juan A. Pérez-Claros [a], Christine M. Janis [b], Darren R. Gröcke [c]

[a] Departamento de Ecología y Geología, Facultad de Ciencias, Campus Universitario de Teatinos, 29071-Málaga, Spain

[b] Department of Ecology and Evolutionary Biology, Brown University, Providence, RI 02912

[c] Department of Earth Sciences, Durham University, Science Laboratories, South Road, Durham DH1 3LE, UK

* Corresponding author. Departamento de Ecología y Geología, Facultad de Ciencias. Campus de Teatinos s/n, E-29071-Málaga. *E-mail address:* ppb@uma.es (P. Palmqvist), *Fax:* (+34) 952137386

## Abstract

Research into the reconstruction of ancient communities in terms of dietary regimes, habitat preferences and ecological interactions of species has focused predominantly on biogeochemistry or ecomorphology alone and not in combination. The Venta Micena site (Orce, Guadix-Baza basin, SE Spain) has an early Pleistocene vertebrate assemblage with exceptional biomolecular preservation. Collagen was successfully extracted from 77 bone samples of 18 species of large mammals, which allowed analyses of carbon- and nitrogen-isotopes. $\delta^{13}C$, $\delta^{15}N$ and $\delta^{18}O$ ratios combined with ecomorphological indexes provide interesting clues on the autecology and palaeophysiology of extinct species, which help in deciphering aspects of community trophic structure and predator-prey interactions. Specifically, morphometric ratios (e.g., hypsodonty index and relative length of the lower premolar tooth row; Palmqvist et al., 2003) allow classifying the ungulates among grazers

(*Equus altidens, Bison* sp., *Praeovibos* sp., *Hemitragus albus, Hippopotamus antiquus,* and *Mammuthus meridionalis*), mized-feeders (*Soergelia minor* and *Pseudodama* sp.) and browsers (*Stephanorhinus* sp. and *Praemegaceros* cf. *verticornis*). However, $\delta^{13}C$ values reveal that these ungulates consumed exclusively $C_3$ plants and significant differences in isotopic values between perissodactyls (monogastric, hindgut fermenters) and ruminants (foregut fermenters) must reflect physiological differences related to their rates of methane production and digestive efficiency. $\delta^{18}O$ ratios allow the interpretation of the dietary water source of these species, suggesting that fallow deer *Pseudodama* sp., goat *H. albus* and ovibovine *S. minor* obtained a significant fraction of their metabolic water from the vegetation consumed. Carnivore species have higher $\delta^{15}N$ values than herbivores, which records the isotopic enrichment expected with an increase in trophic level. However, the unexpectedly high $\delta^{15}N$ values of hippo *H. antiquus* and muskoxen *Praeovibos* sp. suggest that these ungulates predominantly consumed aquatic plants and lichens, respectively. Inferences on predator-prey relationships within this ancient community, derived from the dual linear mixing model, indicate resource partitioning among sympatric predators, suggesting that sabre-tooth *Megantereon whitei* and jaguar *Panthera* cf. *gombaszoegensis* were ambushers of forest environments while sabre-tooth *Homotherium latidens* and wild dog *Lycaon lycaonoides* were coursing predators in open habitat. The giant, short-faced hyena *Pachycrocuta brevirostris* scavenged the prey of these hypercarnivores.

*Keywords:* Mammals; Ecomorphology; Biogeochemistry; Pleistocene; Venta Micena; Orce

## 1. Introduction: the early Pleistocene locality of Venta Micena

Venta Micena lies near the village of Orce (Granada, SE Spain) in the eastern sector of the Guadix-Baza Basin (37º44'15''N, 2º24'9''W, elevation 974.5 m; Fig. 1). This sedimentary basin was characterized by interior drainage from the end of the Miocene to middle-late Pleistocene times, which facilitated the preservation of Plio-Quaternary large mammal assemblages in swampy

and lacustrine sediments. The site is dated by biostratigraphy to the lower Pleistocene (Arribas and Palmqvist, 1999), with an age estimated in ~1.5 Ma.

The Venta Micena stratigraphic column shows alternate micrite limestone, calcilutitic, lutitic, silty, and marly levels (Fig. 1). The main excavation quarry (VM-2 level, Quarry 3 and drillings 1-4, ~320 $m^2$; Palmqvist and Arribas, 2001) is located within the upper part of the section, in an 80-120 cm thick limestone stratum undisturbed by tectonic activity, composed of homogeneous and porous micrite sediments (98-99% $CaCO_3$) that can be followed across ~2.5 km in the Orce area (Arribas and Palmqvist, 1998). The lower half of the stratum has carbonate nodules (5-20 cm thick), mud banks and fossil shells of eurythermal freshwater molluscs. During this lacustrine stage, micrite was precipitated in a shallow (<10 m), well-oxygenated water sheet not subject to eutrophic conditions, as indicated by the absence of pyrite and carbonate facies rich in organic matter. Above this level there is a 4-15 mm thick calcrete palaeosol, which records a major retreat of the Pleistocene lake and represents a swampy biotope with wide emerged zones (~4 km width) and shallow ponds (<1 m depth, 2-20 m diameter). The upper half of the stratum is composed of micrite sediments showing root marks and mud cracks at the bottom, which record the rise of the lake level, and preserves a high density of fossil bones.

The large mammals assemblage is composed of ~5,800 identifiable skeletal remains from 225 individuals belonging to 21 taxa of large (>5 kg) mammals and ~10,000 unidentifiable bone shafts and cranial fragments. Herbivorous taxa dominate the assemblage in number of identifiable specimens (*NISP*) and estimates of minimal number of individuals (*MNI*). The surface of the skeletal remains is not abraded and the longitudinal axes of long bones show no preferred orientation, which indicates that they were not transported by fluvial processes prior to deposition. Furthermore, the ratio of isolated teeth to vertebrae (0.94:1) is close to the value expected in the absence of hydrodynamic sorting (1:1) and the frequencies of bones grouped according to their potential for dispersal by water (i.e., Voorhies's groups) are similar to those in the mammalian skeleton (Arribas and Palmqvist, 1998). Analysis of weathering stages indicates a short time of

exposure before burial, less than one year in most cases. Analysis of mortality patterns deduced for ungulate species from juvenile/adult proportions reveals that most skeletal remains were scavenged by the giant, short-faced hyena *Pachycrocuta brevirostris* from carcasses of animals hunted selectively by hypercarnivores (Palmqvist et al., 1996). Taphonomic analysis shows that the hyenas transported ungulate carcasses and body parts to their maternity dens as a function of the mass of the ungulates scavenged. The fracturing of major limb bones in the dens was also highly selective, correlating well with their marrow contents and mineral densities (Palmqvist and Arribas, 2001).

Palaeoecological analyses include inferences on the life style and preferred habitat of extinct taxa (palaeoautecology) and the reconstruction of past ecological associations (palaeosynecology) (Damuth, 1992). Once the preservational completeness of the fossil assemblage has been evaluated with taphonomic analysis, it is necessary to infer the autecological characteristics of the species prior to synecological analysis at the community level. Autecological properties of extinct taxa may be reconstructed through: 1) ecomorphological inferences on functional adaptations for feeding behaviour and types of locomotion; 2) biogeochemical analyses for reconstructing dietary niches, habitat preferences and palaeotemperatures; and 3) studies of the sedimentary context and taphonomic attributes of the fossils as well as on their distribution across facies (Wing et al., 1992; Palmqvist et al., 2003; Soligo and Andrews, 2005). Once this goal is achieved, species can be distributed among size classes and ecological categories, and the relative frequencies of these categories in the assemblage are compared with those in modern ecosystems (Andrews et al., 1979; Reed, 1998; Mendoza et al., 2005).

Feeding preferences of extinct mammals can be addressed using biogeochemical markers such as stable-isotopes and trace-elements, as well as from the comparative study of their craniodental morphology, because several features of the skull, mandible and dentition are indicative of diet (see reviews in MacFadden, 2000; Williams and Kay, 2001; Mendoza et al., 2002; Palmqvist et al., 2003). In herbivores, the hypsodonty index (*HI,* unworn molar crown height divided by molar width) discriminates between grazers (>75% grass in diet), which feed upon

grasses with high silicophytolith contents and have hypsodont, high-crowned molars, from browsers (<25% grass in diet), which consume succulent leaves and have brachydont, low-crowned teeth. However, although *HI* is probably the best single variable correlated with diet in living ungulates (and thus of the best use for predicting the diet of extinct ones), in some species molar crown height alone may be insufficient to determine their feeding preferences (Fortelius and Solounias, 2000; Mendoza et al., 2002). Muzzle shape also provides information on diet, as it reflects the adaptations related to the "cropping mechanism", including the shape of the premaxilla and the relative proportions of the incisor teeth (Janis and Ehrhart, 1988; Solounias and Moelleken, 1993; Pérez-Barbería and Gordon, 2001): browsers have narrow muzzles consisting of a rounded incisor arcade with the first incisor generally larger than the third, while grazers have broad muzzles with transversely straight incisor arcades, showing equal or sub-equal sized teeth. There are, however, some second-order differences related to the phylogenetic legacy: equids have relatively narrower muzzles than grazing ruminants of similar body size. In addition, different ungulate groups have adopted different solutions when faced with the same ecological specialization: for example, the lower premolars are enlarged in grazing perissodactyls, but grazing ruminants and camelids show the opposite trend. This difference is probably due to differences in the way food is orally processed in foregut and hindgut fermenters (Mendoza et al., 2002).

In carnivores, craniodental features related to diet include the morphology of the upper canine, the size of the trigonid blade and the talonid basin in the lower carnassial, and the shape of the glenoid and angular processes in the mandible, which reflect the moment arms for jaw adductor muscles (Van Valkenburgh, 1988; Biknevicius and Van Valkenburgh, 1996). These variables help in discriminating among hypercarnivores, bone-crackers and omnivores. Relevant features of the postcranial skeleton include the brachial and crural indexes (i.e., radius length divided by humerus length and tibia length divided by femur length, respectively), the ratio of phalanx length to metacarpal length, the biceps brachii leverage index, and cross-sectional geometric properties of major limb bones (Van Valkenburgh, 1985; Anyonge, 1996; Lewis, 1997). These variables estimate

different aspects related to habitat preferences and hunting techniques: for example, the brachial and crural indexes are useful for discriminating between predators that ambush their prey in forested environments and those that pursue it in open habitat (Palmqvist et al., 2003).

## 2. Sedimentary geochemistry and palaeoenvironmental inferences

The trace-element and stable-isotope chemistry of lake waters is a sensitive monitor of climate in arid and semi-arid regions (see review in Hu et al., 1998). Data of trace-element abundance and stable-isotope ratios in the stratigraphic section of Venta Micena (Table 1; Figs. 1A-B) show several key relationships. For example, sodium concentrations decrease systematically from the base of the section, reach their lowest values in the middle of the section, and then suddenly rise to high values below the palaeosoil (Fig. 1A). If sodium concentrations are assumed as representative of lake salinity levels, they show that the middle part of the section witnessed an increase in the water level and/or a reduction of salinity, although the salinity level dramatically increased just prior to palaeosoil development, evidencing the lowering of the water table. Iron and manganese concentrations decrease from level VM-1 to level VM-2, suggesting a shift from a restricted, stratified water column (decreased oxygen levels, stagnation) to a more open, well-oxygenated water column. This evidence supports the increase in lake-level in the middle of the section, as indicated by sodium concentrations, which resulted in increased water supply and, thus, circulation.

Magnesium and strontium concentrations decrease and increase, respectively, through the whole stratigraphic section (Fig. 1A). Magnesium and strontium concentrations are under saturated with respect to the minerals commonly precipitated within lakes and for this reason both elements have been used for reconstructing changes in water lake salinity levels (Chivas et al., 1985). Magnesium also correlates negatively with water temperature (Chivas et al., 1986). However, on the basis of these bulk-rock analyses, a similar assumption would be difficult here, because magnesium and strontium are negatively correlated in the Venta Micena section.

153 Oxygen-isotope analyses of the bulk-rock samples show a general decrease to more negative
154 $\delta^{18}O$ values through the section (Fig. 1B), paralleling the magnesium concentration record. This
155 indicates that magnesium and $\delta^{18}O$ are negatively correlated with the palaeotemperature of the lake
156 waters and, thus, an overall warming from level VM-1 to the development of the palaeosoil at level
157 VM-2. Sodium and strontium concentrations should be negatively correlated if strontium measures
158 palaeosalinity levels, what is not reflected in the Venta Micena section. However, in a
159 palaeohydrochemical study of a nearby early Pleistocene shallow lacustrine section from Orce,
160 Anadón and Julià (1990) found lower Sr/Ca values in ostracod shells from sands deposited during
161 saline water phases than in those from the overlying carbonate sequences formed under lower
162 salinity conditions; such unexpected values were interpreted as the result of major changes in the
163 chemical composition of the water in shallow swamped areas of a hydrologically complex lake. A
164 subsequent study (Anadón et al., 1994) revealed higher $\delta^{18}O$ ratios in ostracod shells from intervals
165 with a saline fauna than in those with a freshwater fauna, what is also recorded in the bulk-rock
166 analyses of the Venta Micena section (Fig. 1B). According to Anadón et al. (1994), this would
167 correspond to an alternation of concentration/dilution phases in a shallow lacustrine sequence that
168 correlates with the climatic cycles described in synchronous ocean basin records from the late
169 Matuyama chron. Anadón et al. (1994) also found a covariant trend in $\delta^{13}C$ and $\delta^{18}O$ values from
170 ostracod calcite, which indicates that the ostracods lived in a closed lacustrine system. $\delta^{13}C$ and
171 $\delta^{18}O$ ratios are also correlated in the Venta Micena section (Fig. 1B).

172 Bulk-rock $\delta^{13}C$ ratios are, however, an archive of more difficult interpretation. They show the
173 maximum value in the marly level at the base of the section, fluctuate in the silty, lutitic and
174 calcilutitic levels placed in the section from 0.85 m to 2.5 m, and then show a slight decrease in the
175 micrite levels (Fig. 1B). Organic residues in modern soils reflect the $\delta^{13}C$ of the overlying flora
176 (Koch, 1998). Because its carbon is derived from soil $CO_2$, the $\delta^{13}C$ of soil carbonate is strongly
177 correlated to that of soil organic matter. Atmospheric $CO_2$ has a higher $\delta^{13}C$ value (–6.5‰) than
178 both $C_3$ plants (–26‰) and $C_4$ plants (–12‰), contributing to soil $CO_2$ near the surface; however,

179 the $CO_2$ >30 cm deep in soils with moderate to high respiration rates is largely supplied by plant
180 decay and root respiration. Both processes generate $CO_2$ isotopically similar to organic matter.
181 Diffusion of $CO_2$ from the soil to the atmosphere leads to a $\delta^{13}C$ enrichment of +4.5‰ for $CO_2$ at
182 depth in a soil relative to soil organic matter. Finally, temperature-dependent fractionation
183 associated with precipitation of calcite sum to a $\delta^{13}C$ increase of +10.5‰ (Koch, 1998). As a
184 consequence, modern carbonates forming below 30 cm depth have $\delta^{13}C$ values ~15‰ higher on
185 average than those of organic matter: –11‰ for soils with $C_3$ overlying flora and +3‰ for soils in
186 which organic matter is supplied by $C_4$ plants (Koch, 1998). The range of $\delta^{13}C$ ratios measured in
187 the Venta Micena stratigraphic section (–4.1‰ to –7.4‰) lies between both values, suggesting a
188 mixed vegetation of $C_3$ and $C_4$ plants. However, $\delta^{13}C$ values for bone collagen of grazing ungulates
189 (see below) show the absence of $C_4$ grasses in their diet. This indicates that other factors apart from
190 changes in primary productivity and respiration in the water column may also have been involved in
191 determining bulk-rock $\delta^{13}C$ ratios; for example, under higher pressures of atmospheric $CO_2$, more
192 of the $CO_2$ at depth in soils would be derived from the atmosphere, increasing the difference in $\delta^{13}C$
193 values between soil carbonate and organic matter (Koch, 1998).

194 In a recent study of a 356-m-thick composite section of the Guadix-Baza basin that ranges
195 from the late Pliocene to the middle Pleistocene, Ortiz et al. (2006) interpreted the $\delta^{13}C$ and $\delta^{18}O$
196 profiles as reflecting changes in temperature, the evaporation/infill ratio in the water bodies and the
197 amount of rain. Specifically, they concluded that high $\delta^{13}C$ and $\delta^{18}O$ values were associated with
198 warm and dry regimes, whereas low $\delta^{13}C$ and $\delta^{18}O$ values correlated with cold and humid episodes,
199 which caused more vegetation biomass and, therefore, an increase in the input of isotopically light
200 carbon.

201 Strontium isotopes ($^{87}Sr/^{86}Sr$) can be used for deriving the palaeosalinity record of ancient
202 environments if independent constraints on the system's hydrologic parameters (i.e., evaporation,
203 precipitation, fluvial and ocean exchange fluxes) are available (e.g., salinity estimates provided by
204 lithology and faunal assemblages; Flecker et al., 2002). $^{87}Sr/^{86}Sr$ ratios of river waters are similar to

205 those of terrestrial plants and there are no significant differences in $^{87}Sr$ contents between grasses
206 and trees (Hoppe et al., 1999). In herbivores, the $\delta^{87}Sr$ value of bioapatite equals the average ratio
207 of the vegetation ingested, which in turn monitors the soluble strontium in soils, derived from
208 weathering and precipitation. Environmental $^{87}Sr/^{86}Sr$ ratios vary with differences in atmospheric
209 input as well as with differences in bedrock age and composition (Price et al., 1985; Miller et al.,
210 1993). Due to this reason, variations in $\delta^{87}Sr$ have been used for reconstructing migratory behaviour
211 in a variety of vertebrates, including proboscideans (Koch et al., 1995; Hoppe et al., 1999; Hoppe,
212 2004). Concerning the stratigraphy of Venta Micena (Fig. 1B), bulk-rock $^{87}Sr/^{86}Sr$ ratios are
213 relatively uniform in the lower part of the section, with the only exception of a decrease in level
214 VM-1. This reflects deposition under conditions of hydrological stability. The upper carbonate
215 samples, however, show a significant decrease in $^{87}Sr/^{86}Sr$ proportions, which reflects an increase in
216 river or groundwater input that translated in the rising of the lake's table in the lacustrine levels.

217 **3. Stable-isotope analyses of the Venta Micena fauna**

218 Stable isotopes have proved useful in determining the dietary niches of extinct mammals,
219 providing detailed ecological and environmental reconstructions. Published carbon-, nitrogen- and
220 oxygen-isotopes of collagen and hydroxylapatite from 18 species of large mammals identified in the
221 Venta Micena assemblage (Gröcke et al., 2002; Palmqvist et al., 2003; N = 65) and results obtained
222 from additional samples (N = 50; Table 2) of juvenile individuals and species not sampled in the
223 previous study (e.g., *Praeovibos* sp., *Hystrix major, Panthera* cf. *gombaszoegensis,* and *Ursus*
224 *etruscus*) are analyzed here to determine their dietary niches and predator-prey relationships.
225 Collagen was successfully extracted from 77 bone samples, which allowed analyses of carbon- and
226 nitrogen-isotopes. Oxygen-isotopes were retrieved from 115 bone and tooth hydroxylapatite
227 samples. The precision for stable-isotope analysis was 0.1‰ for both carbon and oxygen, and 0.2‰
228 for nitrogen. Carbonate carbon and oxygen isotopic analyses were performed using a Fison Optima
229 isotope-ratio mass-spectrometer, with a common acid bath system in the Stable-Isotope
230 Biogeochemistry Laboratory at McMaster University. Samples were reacted with 100% phosphoric

231 acid at 90ºC. Collagen carbon and nitrogen isotopic analyses were performed at the Stable-Isotope
232 Biogeochemistry Laboratory at McMaster University using a Thermo-Finnigan DeltaPlus XP
233 coupled with a Costech elemental analyzer.

234 Stable isotopes are useful palaeobiological tracers because, as a result of mass differences,
235 different isotopes of an element have different thermodynamic and kinetic properties, leading to
236 measurable isotopic partitioning during physical and chemical processes, which labels the
237 substances with distinct isotopic ratios (Gröcke, 1997a; Koch, 1998). Isotopic ratios are reported as
238 parts per thousand (‰) of deviation from a standard, using the δ notation, where:

239 $$\delta X = [(R_{sample} / R_{standard}) - 1] \cdot 1000,$$

240 where, X = C, N or O, and R = $^{13}C/^{12}C$, $^{15}N/^{14}N$ or $^{18}O/^{16}O$. $R_{sample}$ and $R_{standard}$ are the high-mass to
241 low-mass isotope ratios of the sample and the standard, respectively. Common standards for $\delta^{13}C$,
242 $\delta^{15}N$ and $\delta^{18}O$ are Peedee belemnite (PDB), atmospheric $N_2$ and standard mean ocean water
243 (SMOW), respectively.

244 The measurement of carbon- and nitrogen-isotope ratios in an animal's bone collagen provides
245 an indication of aspects of its overall diet for the last few years of life (De Niro and Epstein, 1978).
246 Apart from a report on bone collagen preserved in Late Cretaceous dinosaurs (Ostrom et al., 1993),
247 original carbon- and nitrogen-isotope compositions have been retrieved from organic residues in
248 fossils as old as 200 ka (Jones et al., 2001), though adequate preservation in such ancient specimens
249 is rare (Bocherens et al., 1996a; Gröcke, 1997a). Thus, the extraction of collagen from 77 out of 105
250 fossil bone samples of Venta Micena, a locality with an age of ~1.5 Ma, constitutes an example of
251 unusual biomolecular preservation. It is worth mentioning that other fossil proteins (e.g., albumin
252 and immunoglobin) have also been detected in fossil samples from this site using immunological
253 techniques (Torres et al., 2002).

254 Several methods are available to identify alteration of collagen, including analysis of C:N
255 ratios (between 2.9 and 3.6) and amino acid composition (Gröcke, 1997a; Richards et al., 2000;

Drucker et al., 2003). These criteria allow for the identification and exclusion of collagen that is heavily degraded and/or contaminated. This is not the case at Venta Micena, because C:N ratios of the collagen material extracted averaged 3.18 (Table 2) and the amino acid composition from four specimens is similar to that of bone collagen in modern mammals, indicating good preservation (Palmqvist et al., 2003; Fig. 6).

*3.1. Carbon-isotopes and palaeodiet*

Terrestrial plants can be divided into two main groups on the basis of their photosynthetic pathway (Edwards and Walker, 1983): 1) $C_3$ plants, which follow the Calvin-Benson cycle (atmospheric $CO_2$ is fixed through the reductive pentose phosphate pathway); and 2) $C_4$ plants, which use the Hatch-Slack cycle ($C_4$-dicarboxylic acid pathway). $C_3$ plants are all trees and bushes, temperate shrubs and grasses adapted to cool/moist climate and/or high altitude, whereas $C_4$ plants include tropical, arid-adapted grasses. All plants take up $^{12}CO_2$ in preference to $^{13}CO_2$, but are important differences in their isotopic composition related to their carboxylating enzymes (Smith and Epstein, 1971; Gröcke, 1997b; Koch, 1998). $C_3$ plants use the ribulose carboxylase and have an average $\delta^{13}C$ value of –26.0 ± 2.3‰ (range: from –35‰ in closed canopy to –20‰ in open areas exposed to water stress). $C_4$ plants use the phosphoenolpyruvate carboxylase, which discriminates less effectively against $^{13}CO_2$, showing a mean $\delta^{13}C$ value of –12.0 ± 1.1‰ (range: –19‰ to –8‰).

When plants are consumed by herbivores, the plant carbon is incorporated into their skeletal tissues with some additional fractionation. The difference between the $\delta^{13}C$ value of the animal's diet and that subsequently incorporated into bone collagen ($\delta^{13}C_c$) translates in an average increase per trophic level of +1.0‰ (range: 0‰ to +4.5‰) and a similar enrichment is recorded in carnivores (see review in Bocherens and Drucker, 2003). The isotope enrichment factor for biogenic apatite is higher, +14.1‰ on average for ungulates (Cerling et al., 2003).

279 *3.2. Nitrogen-isotopes and trophic level*

280 The nitrogen-isotope composition of collagen in mammals records their position in the trophic
281 web, since each trophic level above herbivore is indicated by a mean increase in $\delta^{15}N$ of ~3.4‰
282 (range: 1.7‰ to 6.9‰; Robinson, 2001; Bocherens and Drucker, 2003; Vanderklift and Ponsard,
283 2003). Soil synthesis of nitrogen, the diet of the animal (i.e., if it consumes $N_2$-fixing or non-$N_2$-
284 fixing plants) and nitrogen metabolism are the primary factors that affect the $\delta^{15}N$ value expressed
285 in herbivore collagen (Sealy et al., 1987; Virginia et al., 1989; Bocherens et al., 1996b; Gröcke et
286 al., 1997; Koch, 1998; Robinson, 2001). Herbivores from closed environment show lower $\delta^{15}N$
287 values than those from open grassland because of soil acidity in dense forest. Plants that fix
288 nitrogen have $\delta^{15}N$ values that cluster close to the atmospheric $N_2$ value of 0‰, whereas those that
289 do not fix nitrogen and use other sources (e.g., soil $NH_4^+$ and $NO_3^-$) show a wider range of values.
290 Therefore, animals consuming $N_2$-fixing plants will generally exhibit $\delta^{15}N$ values between 0‰ and
291 4‰, while herbivores feeding on non-$N_2$-fixing plants will show $\delta^{15}N$ values comprised between
292 2‰ and 8‰. Plants near marine or salt-affected areas show enrichment in $\delta^{15}N$ values and deep-
293 rooted plants are enriched over those with shallow roots.

294 The effects of nitrogen metabolism in mammals are very important. Higher $\delta^{15}N$ values are
295 observed in mammals inhabiting arid regions, due to ecophysiological differences in nitrogen
296 metabolism associated with adaptations for drought tolerance: under conditions of increased aridity,
297 mammals concentrate urine and excrete concentrated urea, subsequently causing elevated $\delta^{15}N$
298 values (Gröcke, 1997a; Koch, 1998; Schwarcz et al., 1999). In general, higher $\delta^{15}N$ values are
299 found in perissodactyls (monogastric, hindgut-fermenting herbivores) than in foregut ruminants
300 (Gröcke and Bocherens, 1996), but the cause behind these elevated values is not clearly understood.
301 Ruminants have a distinct process of nitrogen cycling, where some waste urea is dumped into the
302 rumen, and they are thus less water dependent than monogastric herbivores. Elevated $\delta^{15}N$ levels

303 may also be indicative of young suckling animals, due to the ingestion of nutrient-enriched milk
304 (Gröcke, 1997a; Jenkins et al., 2001).

305 *3.3. Oxygen-isotopes and water requirements*

306 Oxygen-isotope values in enamel and bone apatite reflect prevailing climatic conditions (e.g.,
307 palaeotemperature; Koch et al., 1989; Ayliffe et al., 1992), but they also allow the interpretation of
308 the dietary water source of a local fauna (Sponheimer and Lee-Thorp, 2001; Harris and Cerling,
309 2002). The oxygen-isotope composition of apatite is a function of three main oxygen sources:
310 atmospheric $O_2$, liquid water and oxygen bound in food (Bryant and Froelich, 1995; Bryant et al.,
311 1996; Kohn, 1996; Kohn et al., 1996). Unlike atmospheric $O_2$, the $\delta^{18}O$ composition of food and
312 water are highly variable, and thus likely to explain any differences found in the $\delta^{18}O$ ratios of
313 sympatric taxa. The $\delta^{18}O$ in plants is more positive than in their source water, which is ultimately
314 derived from local rain. In most cases, liquid water in plant roots and stems is isotopically similar to
315 drinking water available for herbivores, but leaf water is relatively enriched in $H_2{}^{18}O$ due to
316 preferential evapotranspiration of the lighter $H_2{}^{16}O$ molecule. A study of the oxygen isotope
317 composition of modern South African ungulates (Sponheimer and Lee-Thorp, 2001) revealed that
318 mixed-feeding impalas (*Aepyceros melampus*), grazing tsessebes (*Damaliscus lunatus*) and blue
319 wildebeests (*Connochaetes taurinus*) obtain relatively more of their water from green vegetation
320 and are significantly enriched in $^{18}O$ compared to other herbivores such as warthog (*Phacochoerus*
321 *aethiopicus*), waterbuck (*Kobus ellipsiprymmus*) and giraffe (*Giraffa camelopardalis*), which derive
322 more of their total water intake from drinking. Similar differences were detected by Harris and
323 Cerling (2002) between grazing and browsing East African ungulates. Thus, among extinct
324 ungulates a more positive result would indicate that the species obtained most of its water
325 requirements from the plants eaten rather than from drinking. Animal tissues consist mainly of
326 proteins whereas plant tissues consist mainly of carbohydrates. Given that proteins are depleted in
327 $^{18}O$ compared to carbohydrates, carnivores show lower $\delta^{18}O$ values than herbivores (Sponheimer
328 and Lee-Thorp, 2001).

## 4. Trophic level and palaeodietary inferences

Figure 2 shows a plot of $\delta^{13}C$ and $\delta^{15}N$ values measured in large mammals from Venta Micena. The range of $\delta^{13}C$ values for ungulates (–27‰ to –20‰) agrees with that of modern herbivores eating $C_3$ plants, which confirms that $C_4$ grasses were absent from southern Spain during early Pleistocene times (Palmqvist et al., 2003). There are, however, important variations of carbon-isotope ratios among ungulates (Fig. 3), with perissodactyls showing the lowest $\delta^{13}C$ values (range: –26.7‰ to –24.2‰) and bovids the highest ones (range: –23.9‰ to –20.1‰). This difference is statistically significant ($t$ = 19.25, $p < 0.0001$) and does not seem to indicate a different feeding behaviour for both groups, given their hypsodonty values (*HI*). In fact, the two perissodactyl species have similar $\delta^{13}C$ values, but the highly hypsodont cheek teeth (*HI* = 6.1) of horse *Equus altidens* identify it as a grazer (*HI* = 3.9-8.7 for grazing perissodactyls; Mendoza *et al.,* 2002), whereas the brachydont teeth (*HI* = 1.8) of rhino *Stephanorhinus* sp. indicate that it was a mixed feeder or browser (*HI* = 0.8-2.2 for mixed-feeding and browsing perissodactyls; Mendoza et al., 2002). Both species presumably inhabited open, relatively unforested environments, given their comparatively high $\delta^{15}N$ values (Fig. 3). Among the bovids, the bovine *Bison* sp. (*HI* = 3.9) and the caprine *Hemitragus albus* (*HI* = 4.4) have moderately hypsodont teeth, indicative of a diet composed mainly of grass (*HI* = 3.8-6.1 for modern grazing bovids; Mendoza et al., 2002). In contrast, the ovibovine *Soergelia minor* has mesodont teeth (*HI* = 2.9), suggestive of a mixed diet (*HI* = 2.5-5.3 for mixed-feeding bovids from open habitat; Mendoza et al., 2002). The relatively high $\delta^{15}N$ values of all these extinct bovids suggest that they dwelled in unforested environments. Cervids *Praemegaceros* cf. *verticornis* and *Pseudodama* sp. also show lower $\delta^{13}C$ mean ratios than bovids (–25.9‰ to –22.2‰) ($t$ = 11.71, $p < 0.0001$, two-tailed test). Both species have low-crowned teeth (*HI* = 1.6 and 1.7, respectively), which suggests that they were mixed feeders or browsers in closed habitat, as most cervids (*HI* = 1.1-2.8 in modern deer; Mendoza et al., 2002). In fact, *P. verticornis* shows the lowest $\delta^{15}N$ contents among ungulates and lower $\delta^{13}C$ values than other ruminants (Fig. 3), which suggests a browsing diet in closed canopy.

355 The similarity in $^{13}C/^{12}C$ ratios shown by the two perissodactyls is unlikely to indicate
356 similarity in diets, and shared dietary differences to the ruminants, especially as there were no $C_4$
357 grasses in this locality. Rather, it reflects a lower isotope enrichment factor for the heavy-carbon
358 isotope in these monogastric herbivores than in ruminants, related to physiological differences
359 between both groups in their digestive systems (hindgut and foregut, respectively). Of interest for
360 this study, Cerling and Harris (1999) found that Burchell's zebras (*Equus burchelli*), whose diet is
361 composed of nearly 100% grass (McNaughton and Georgiadis 1986), are consistently 1-2‰
362 depleted in $\delta^{13}C$ values for tooth enamel compared to sympatric ruminant hypergrazers such as
363 alcelaphine bovids; this depletion implies a lower isotope enrichment factor for zebras, resulting
364 from their lower digestive efficiency. A similar difference was detected by Lee-Thorp and Van der
365 Merwe (1987) between bone bioapatite samples from zebra and wildebeest (*Connochaetes*
366 *taurinus*). Recent studies of bone collagen isotopes of European fauna over the last glacial cycle and
367 the Holocene also showed consistently 1-2‰ depleted $\delta^{13}C$ values in horse compared to ruminants
368 (Bocherens and Drucker, 2003; Richards and Hedges, 2003). However, it is worth noting that the
369 difference in $\delta^{13}C$ ratios between ruminants and perissodactyls in Venta Micena is greater than the
370 differences reported at other sites, which suggests that some dietary differences must be also
371 involved.

372 The two megaherbivores, elephant *Mammuthus meridionalis* and hippo *Hippopotamus*
373 *antiquus,* show high $\delta^{13}C$ values, similar to those of bovids (Fig. 3). The proboscidean seems to
374 have been a mixed feeder like modern African elephants (*Loxodonta africana*), although grass
375 probably was a more significant component of its diet according to carbon-isotopes of tooth enamel
376 in fossil *Mammuthus* from Africa and North America (Koch et al., 1998; Cerling et al., 1999). In the
377 case of *H. antiquus,* the modern hippo, *Hippopotamus amphibious,* is a reputedly grazer that has
378 brachydont teeth, as in the specimens of Venta Micena. The reason for this apparent anomalous
379 condition of low hypsodonty is most likely related to the fact that hippos have low metabolic rates,
380 consuming less food per day than would be expected for animals of their size (Novak, 1999;

381 Schwarm et al., 2006), which translates in a lower amount of wear on the teeth (Mendoza et al.,
382 2002). In addition, a recent study of the isotopic composition of enamel in several African
383 populations of *H. amphibious* has shown that modern hippos have a more varied diet than usually
384 thought, including significant amounts of $C_3$ plants in closed to moderately open environments
385 (Boisserie et al., 2005).

386 The higher $\delta^{13}C$ enrichment of the Venta Micena ruminants, in comparison with the
387 perissodactyls, is probably related to the higher rates of methane production in the forestomach of
388 ruminants than in the hindgut of monogastric herbivores, which derive a lower fraction of
389 maintenance energy from methanogenetic activity of bacteria (Crutzen et al., 1986; Vermorel et al.,
390 1997; Schulze et al., 1998; Metges et al., 1990; Hedges, 2003). However, it seems anomalous that
391 the elephant, a hindgut fermenter, should have an enrichment value that resembles that of the
392 ruminants. However, elephants are not closely related to perissodactyls (Springer et al., 1997) and
393 phylogenetic differences may be at work here. In addition, elephants have a shorter and wider small
394 intestine in comparison to other hindgut fermenters, which is related to the need for animals of such
395 large size to have a very rapid passage rate of the ingesta (Clauss et al., 2003).

396 The ruminant type of forestomach fermentation provides a clear advantage under conditions
397 of limiting quantities of food: ruminants are very efficient at extracting maximum amounts out of
398 the cellulose and cell contents of food of moderate fibre content, and if feeding on food of relatively
399 good quality they can subsist on a lesser amount of food per day (~70%) than a hindgut fermenter
400 of similar size, which relies on a rapid passage time and the processing of large quantities of food
401 (Janis, 1976; Janis et al., 1984; Duncan et al., 1990). If food is not a limiting factor, however,
402 hindgut fermentation works well with plants of low nutritive value, such as herbage with high fibre
403 contents. This is because a large volume of food can be processed rapidly and the monogastric
404 herbivore can obtain a large quantity of energy from the cell contents in a short time. Among
405 present-day ungulates, the mid range of body sizes (10–1000 kg) is dominated by ruminants. The
406 exceptions are equids, which can feed on low quality grasses too fibrous for a ruminant to subsist

on, and tapirs, which have remained as a relict group of tropical forest browsers. There are physiological reasons behind the absence of ruminants at very small body sizes: given that the basal metabolic rate scales allometrically to the 0.75 power of body mass (and a similar exponent applies to food intake rate in herbivores), small animals have relatively greater energetic demands than larger ones (Kleiber, 1975; McNab, 1986; Shipley et al., 1994). Ruminants less than 10 kg (tragulids and duikers) eat primarily non-fibrous food items, such as young leaves, buds, seeds and fruit, and the small herbivores that can subsist on more fibrous diets are all hindgut fermenters such as hyraxes and lagomorphs. Physiological scaling effects also operate at the largest body sizes: as the retention time of food in the digestive tract scales to the 0.27 power of body mass (Illius and Gordon, 1992), there is no advantage to foregut fermentation above a certain body mass (600 kg for browse, 1200 kg for grass forage) in terms of digestive efficiency, because the retention times and percentages of fibre digestibility are similar for both foregut and hindgut fermenters (Demment and Van Soest, 1985; Prins and Kreulen, 1991; Justice and Smith, 1992; Van Soest, 1994). In addition, while specific metabolic rate decreases with increasing mass, gut capacity remains a constant fraction of body size (Bell, 1971; Jarman, 1974; Geist, 1974; Parra, 1978; Justice and Smith, 1992). This implies that larger ungulates are able to support their lower specific metabolic requirements by ingesting forage of lower quality (Van Soest, 1996). Ruminants are at a disadvantage at very large body sizes, as they are unable to accelerate the passage rate of their ingesta, and may suffer from other physiological problems such as a decreased capacity for water retention (Clauss et al., 2003). The observation on the upper size limit for ruminants, based on the range of modern forms, is supported by the fossil record on extinct ruminants and tylopods, which did not, with the possible exception of the sivatheriine giraffids and some Pliocene North American camels, surpass extant species in maximum body size.

The digestive physiology of elephants, however, deviates from the common scheme postulated for herbivores of increasing body mass (Clauss et al., 2003; Loehlein et al., 2003): elephants do not have long ingesta passage rates and achieve only comparatively low digestibility

433 coefficients. As discussed above, the main nutritional advantage of large body size is that larger
434 animals have lower relative energy requirements and that, due to their increased gastrointestinal
435 tract capacity, they achieve longer ingesta passage rates, which allows them to use forage of lower
436 quality. However, the fermentation of plant material cannot be optimized endlessly, because there is
437 a time when plant fibre is totally fermented and energy losses due to methanogenic bacteria become
438 punitive (Clauss et al., 2003). Therefore, very large herbivores need to evolve adaptations for a
439 comparative acceleration of ingesta passage. Among the extant ungulates, elephants, with their
440 shortened gastrointestinal tract and reduced caecum, are indicators of a trend that allowed even
441 larger hindgut fermenting mammals to exist (Clauss et al., 2003). Foregut fermenting ungulates did
442 not evolve species in which the intake-limiting effect of the foregut could be reduced (e.g., by
443 special bypass structures), and hence their digestive model imposed an intrinsic body size limit for
444 ruminants. This limit will be lower the more the diet enhances the ingesta retention and hence the
445 intake-limiting effect: due to the mechanical characteristics of grass, grazing ruminants cannot
446 become as large as the largest browsing ruminant, the giraffe. In contrast, the design of the
447 gastrointestinal tract of hindgut fermenters allows adaptations for relative passage acceleration,
448 which explains why the largest extinct mammal (*Paraceratherium,* with a body mass of 10,000-
449 15,000 kg; Fortelius and Kappelman, 1993) was a hindgut fermenter (Clauss et al., 2003).

450 Figure 3 shows $\delta^{15}N$ values for the large mammals from Venta Micena. Carnivores
451 *Homotherium latidens, Megantereon whitei, Panthera* cf. *gombaszoegensis, Pachycrocuta*
452 *brevirostris, Lycaon lycaonoides,* and *Canis mosbachensis* show higher values than ungulates
453 except in the case of *H. antiquus* and the sample analyzed of the single specimen of muskoxen,
454 *Praeovibos* sp., preserved in the assemblage. The isotopic fractionation between carnivores and
455 herbivores is in accordance with the enrichment value expected from increasing one trophic level,
456 indicating that the collagen extracted from the fossils did not undergo diagenetic alteration.

457 With the only exceptions of hippo and muskoxen, all ungulate species record isotopic values
458 that agree well with a diet of $N_2$-fixing plants (Fig. 3). The high $\delta^{15}N$ values obtained for *H.*

459 *antiquus,* which are even more elevated than those of the Venta Micena carnivores, suggest that this
460 extinct hippo fed predominantly on aquatic plants, instead of consuming terrestrial grasses as do
461 living hippos (Boisserie et al., 2005). Sealy et al. (1987) found $\delta^{15}N$ values in *H. amphibious* similar
462 to those of other sympatric grazing artiodactyls from southern Africa that feed on terrestrial
463 vegetation, and smaller than those in carnivores. The unexpected diet of *H. antiquus* probably
464 relates to the huge size of this extinct hippo: preliminary estimates based on the diaphyseal diameter
465 of major limb bones provide a figure of ~3200 kg of average body mass for *H. antiquus* (1500 kg
466 for *H. amphibius;* Novak, 1999). In addition, *H. antiquus* had shorter metapodials than modern
467 hippos. Given the fact that *H. amphibius* is not well designed for dwelling on land, the enormous
468 size and short limbs of *H. antiquus* must have posed even more severe limitations for terrestrial
469 locomotion.

470 Modern muskoxen (*Ovibos moschatus*) are sexually dimorphic ruminants that live in a highly
471 seasonal environment, consuming willow, forbs and sedge-dominated vegetation types (Klein and
472 Bay, 1994). However, during winter muskoxen subsist primarily on lichens and some senescent
473 browse. Lichens, although potentially high in digestible energy, contain less protein than required
474 for metabolic maintenance. Thus, the elevated $\delta^{15}N$ value of the single specimen of *Praeovibos* sp.
475 (Fig. 3) could indicate increased recycling of nitrogen from body protein during winter due to a
476 poor quality diet (Barboza and Reynolds, 2004; Parker et al., 2005).

477 Perissodactyls and bovids show more positive $\delta^{15}N$ ratios than cervids ($t = 7.36$, $p < 0.05$)
478 (Fig. 3). This indicates that the cervids would preferably feed in closed habitats, where their low
479 $\delta^{15}N$ values would result from soil acidity (Rodière et al., 1996; Gröcke, 1997a). Among the
480 perissodactyls, the comparatively high $\delta^{15}N$ values of the browsing rhino, *Stephanorhinus* sp.,
481 suggest that this species lived in open habitat, in a similar fashion to the modern black rhino
482 (*Diceros bicornis*). $\delta^{15}N$ values for elephant, *M. meridionalis,* are similar to those expected in a
483 large monogastric herbivore (Gröcke and Bocherens, 1996). $\delta^{15}N$ values for the horse, *E. altidens*,
484 are also congruent with those of hindgut fermenters of medium size living in an open environment.

485 Carbon and nitrogen isotopic compositions of collagen provide a proxy to reconstruct ancient
486 trophic webs and especially to decipher the relationships between predators and their potential prey
487 (see review in Bocherens and Drucker, 2003). The wide range of $\delta^{13}C$ and $\delta^{15}N$ values in the Venta
488 Micena carnivores reflects resource partitioning among sympatric predators (Figs. 2-3). For
489 example, sabre-tooth cats *H. latidens* and *M. whitei* have quite distinct isotopic signatures, the
490 former showing the highest $\delta^{13}C$ values among carnivores and the latter the lowest ones (Fig. 3).
491 This suggests that both predators specialized on different types of ungulate prey, which is
492 confirmed by differences in their postcranial anatomy (Anyonge, 1996; Arribas and Palmqvist,
493 1999; Palmqvist and Arribas, 2001; Palmqvist et al., 2003). The dirk-tooth *M. whitei* had a robust
494 body, a low brachial index (~80%) and short metapodials, features that describe it as an ambush
495 predator of forested habitat. In such an environment, browsing ungulates with depleted $\delta^{13}C$ and
496 $\delta^{15}N$ values would have been the preferred prey. The European jaguar *P. gombaszoegensis* was also
497 an ambusher with a postcranial anatomy similar to that of the extant jaguar (*Panthera onca*). The
498 scimitar-tooth *H. latidens* had comparatively long and slender limbs, and a body size similar to that
499 of a modern lion (*Panthera leo*). The forelimb was more elongated than the hind limb, indicating
500 that the animal probably had a sloping back. This suggests adaptations to carry away large prey.
501 The claws of *Homotherium* were small, with the exception of a well-developed dewclaw in the first
502 digit of the forefoot. The elongated forelimb (brachial index of ~100%) and small claws suggest
503 increased cursoriality in an open habitat and less prey grappling capability than other sabre-tooth
504 cats (Palmqvist et al., 2003). In such habitat, the prey would be large grazing ruminants and
505 juveniles of megaherbivores, as discussed in depth below.

506 Canids *L. lycaonoides* and *C. mosbachensis* show intermediate $\delta^{13}C$ values, while the hyena
507 *P. brevirostris,* the bone-collecting agent at this locality, has the highest $\delta^{13}C$ values among
508 carnivores. Results obtained in a comparative ecomorphological study of the craniodental anatomy
509 of modern and Pleistocene canids (Palmqvist et al., 1999, 2002) indicate that the larger canid, *L.*
510 *lycaonoides,* was a hypercarnivore (>70% vertebrate flesh in diet). The postcranial anatomy of this

511 species is similar to that of African hunting dogs (*Lycaon pictus*), the only living canids with a
512 tetradactyl forelimb, which indicates a coursing behaviour. The medium-sized canid, *C.*
513 *mosbachensis,* has a craniodental anatomy similar to those of modern coyote (*Canis latrans*), with a
514 talonid basin well-developed in the lower carnassial. This suggests an omnivorous diet. The short-
515 faced hyena, *P. brevirostris,* had a body and skull 20% larger than in modern spotted hyenas
516 (*Crocuta crocuta*) and was well-adapted for destroying carcasses and consuming bones (Arribas
517 and Palmqvist, 1998; Palmqvist and Arribas, 2001). This hyaenid differed from other species in the
518 shortening of the distal limb segments, which suggests less coursing abilities, although such
519 shortening would provide greater power and more stability for dismembering and carrying large
520 pieces of ungulate carcasses (Turner and Antón, 1996).

521 The high $\delta^{18}O$ values of cervid *Pseudodama* sp., bovids *H. albus* and *S. minor,* and bear *U.*
522 *etruscus* (Fig. 4) suggest that these species obtained most of their water requirements from the
523 vegetation rather than from drinking. In contrast, *M. meridionalis, H. antiquus, Stephanorhinus* sp.,
524 *P. verticornis,* and *Praeovibos* sp. exhibit the lowest $\delta^{18}O$ ratios, which indicate greater water
525 dependence for these species. *Bison* sp. and *E. altidens* show intermediate $\delta^{18}O$ values but closer to
526 those of megaherbivores and large deer, which suggest moderate water dependence for both grazing
527 species. These results agree with expectations from their living closest relatives (see review in
528 Palmqvist et al., 2003). For example, goats are well-adapted for arid conditions, obtaining most of
529 their water requirements from the vegetation; such physiological specialization seems to have been
530 developed by the caprine *H. albus* and the ovibovine *S. minor*. Modern fallow deer (*Dama dama*)
531 tolerates more arid conditions than red deer (*Cervus elaphus*), showing a lower water intake rate per
532 kg of body mass, and this was clearly the case for *Pseudodama* sp. The largest monogastric
533 mammals from Africa, black rhino, hippo and elephant, show a greater water dependence than
534 grazing ruminants (Bocherens et al., 1996a), which agrees with the low $^{18}O$ contents of
535 *Stephanorhinus, Hippopotamus* and *Mammuthus,* respectively. In fact, Harris and Cerling (2002)
536 found that tooth enamel samples from hippos and elephants from Queen Elizabeth Park, Uganda,

were consistently depleted in $^{18}O$ compared with those from $C_4$-grazing ungulates that obtain most of their water from the plants. All carnivore species in Venta Micena show depleted $\delta^{18}O$ values in comparison with the herbivores, as would be predicted from the higher protein content of their diet (Sponheimer and Lee-Thorp, 2001).

## 5. Predator-prey relationships

The differences in $\delta^{13}C$ and $\delta^{15}N$ values among carnivores (Figs. 2-3) suggest specific predator-prey relationships in this early Pleistocene community (Palmqvist et al., 1996). For example, *H. latidens* shows the highest $\delta^{13}C$ and $\delta^{15}N$ values among hypercarnivores, which would indicate that this was the top predator of the palaeocommunity (i.e., the only one able to hunt on very large prey such as juveniles of megafauna and adult ungulates of medium-to-large size). In contrast, *M. whitei* and *P. gombaszoegensis* show the lowest $\delta^{13}C$ and $\delta^{15}N$ ratios, which may provide evidence that browsing ungulates from forest represented an important fraction of their diet.

Previous studies indicate that primary and secondary productivities of the large mammal fauna from Venta Micena assemblage are balanced, which suggests that all large carnivore species living in the original community were preserved in the bone assemblage collected by the hyenas (Palmqvist et al., 2003). Thus, it seems quite reasonable to assume that the potential prey species for each predator were also preserved in the taphocoenosis. The issue here is to assign the preferred ungulate preys to each predator and to quantify their relative contributions to the predator's diet.

Given that the only sources of carbon and nitrogen for a carnivore come from its diet, the composition of its tissues will be a function of what the animal ate. Using the isotopic enrichment from prey to predator and the principle of mass balance, the dual linear mixing model (Phillips, 2001) allows estimating quantitatively the proportional contribution of several ungulate prey species to the diet of a carnivore. For two isotopes and three prey sources, their relative abundances in the diet of a predator consuming them may be estimated from the following equations:

$$\delta^{13}C_{predator} = f_A\,\delta^{13}C'_{prey\,A} + f_B\,\delta^{13}C'_{prey\,B} + f_C\,\delta^{13}C'_{prey\,C},$$

562 $$\delta^{15}N_{predator} = f_A\,\delta^{15}N'_{prey\,A} + f_B\,\delta^{15}N'_{prey\,B} + f_C\,\delta^{15}N'_{prey\,C},$$

563 $$1 = f_A + f_B + f_C,$$

564 where $\delta^{13}C'_{prey}$ and $\delta^{15}N'_{prey}$ are the carbon- and nitrogen-isotope ratios of prey after correction for
565 trophic fractionation, and *f* represents the relative contributions of preys *A, B* and *C* to the diet of
566 predator, respectively. This model has been satisfactorily applied to studies of the diet of living
567 carnivores (Phillips, 2001; Phillips and Koch, 2002; Phillips and Gregg, 2003) as well as to derive
568 inferences on the diet of extinct species, including Neanderthals and anatomically modern humans
569 (Drucker and Bocherens, 2004; Bocherens et al., 2005; Phillips et al., 2005). If an apparently
570 unreasonable solution is obtained for the contribution of a given prey species (i.e., $f < 0$ or $> 1$), this
571 can mean either that an important food source was not included in the analysis or that trophic
572 correction factors were not estimated appropriately (Phillips, 2001). However, the model will yield
573 correct results if some of the sources are not in the predator's diet and even can be used for
574 investigating the dietary composition of a mixture of more than 'n+1' sources for 'n' isotopes
575 (Phillips and Gregg, 2003; Bocherens et al., 2005).

576 This methodological approach was applied to the four hypercarnivore species identified at
577 Venta Micena, *H. latidens, M. whitei, P. gombaszoegensis,* and *L. lycaonoides*. The giant hyena, *P.*
578 *brevirostris,* was excluded from the analysis because taphonomic studies unequivocally indicate
579 that it scavenged the prey of hypercarnivores (Palmqvist et al., 1996; Arribas and Palmqvist, 1998;
580 Palmqvist and Arribas, 2001). The Etruscan bear, *U. etruscus,* was not considered because its teeth
581 are similar to those of modern brown bears (*Ursus arctos*), which is evidence of an omnivorous
582 diet. The craniodental anatomy of the medium-sized canid, *C. mosbachensis,* indicates a more
583 omnivorous behaviour than that of the hunting dog *L. lycaonoides* (Palmqvist et al., 1999, 2002)
584 and was also excluded from subsequent analyses. The comparatively low $\delta^{15}N$ values of this
585 coyote-like species suggest that invertebrates and fruit were also an important fraction of its diet.
586 However, in the case of the bear, its very high $\delta^{15}N$ values are intriguing. Perhaps this species

587 consumed regularly fish, in contrast with the other carnivores, or the high $\delta^{15}N$ values may have
588 resulted from the physiology of dormancy: Fernández-Mosquera et al. (2001) have reported higher
589 $\delta^{15}N$ values in cave bears (*Ursus spelaeus*) that lived during colder periods, which suggest a reuse
590 of urea in synthesizing amino acids with prolonged duration of dormancy.

591 Among ungulates, *H. antiquus* was discarded as a potential prey given its enormous size and
592 amphibious behaviour, which makes it difficult to conceive of a predator specializing on it; the
593 scarce remains of this species in the assemblage would be the result of the scavenging activity of
594 hyenas on carcasses of adult animals dead by other causes than predation and juveniles hunted
595 occasionally by sabre-tooth cats (Fig. 7B). Elephant *M. meridionalis,* however, was analyzed
596 because isotopic data were available for young individuals, the only age stage that would be
597 susceptible to predation according to data on lion predation on modern elephants (see review in
598 Palmqvist et al., 1996). Finally, *Praeovibos* sp. was discarded because this species, poorly
599 represented in the assemblage, presumably lived in mountainous areas, as modern muskoxen.

600 The first step is to quantify the trophic fractionation ($\Delta\delta^{13}C$, $\Delta\delta^{15}N$) between diet and animal
601 tissues, which not an easy task given that enrichment values depend on the type of food sources and
602 animal tissues analyzed. Trophic fractionation in mink and bear range from –2.2 to 4.9‰ for $\delta^{13}C$,
603 and from 2.3 to 4.1‰ for $\delta^{15}N$, respectively (Phillips and Koch, 2002). In a review of studies
604 developed under experimental conditions on isotopic enrichment between diet and collagen,
605 Bocherens and Drucker (2003) found that the enrichment factor ranges from 3.7‰ to 6.0‰ for
606 carbon and from 1.7‰ to 6.9‰ for nitrogen, respectively. These data agree with the commonly
607 quoted ranges for enrichment values of bone collagen of 0 to 2‰ for carbon and 3 to 5‰ for
608 nitrogen. Figure 5 shows the distribution of differences in $\delta^{13}C$ and $\delta^{15}N$ mean values for bone
609 collagen between carnivores and their potential ungulate prey in a set (N = 18) of modern
610 ecosystems and fossil assemblages compiled from the literature. Dentine collagen was not
611 considered here because it tends to show higher $\delta^{15}N$ values than bone collagen in some species,
612 probably due to a suckling isotopic signal retained in dentine and eliminated in bone (Bocherens et

613 al., 2001). Although the range of $\Delta\delta^{13}C$ and $\Delta\delta^{15}N$ values in these communities is very wide (Fig.
614 5), the mean fractionations (1.6‰ and 3.9‰, respectively) are close to those reported previously
615 (Phillips and Koch, 2002; Bocherens and Drucker, 2003).

616 In the case of Venta Micena, the $\Delta\delta^{13}C$ and $\Delta\delta^{15}N$ values between herbivores and carnivores,
617 weighted according to NISP values, are 0.8‰ and 2.8‰, respectively. Given that both values are
618 close to the modal classes in the reference dataset (Fig. 5), they were used for correcting the $\delta^{13}C$
619 and $\delta^{15}N$ values of ungulate prey prior to applying the dual linear mixing model to hypercarnivores.
620 It could be argued, however, that it is circular to apply fractionations calculated from the fossil
621 animals whose diets are being reconstructed. However, this is the most reasonable solution, because
622 in this way the centroids for herbivores and carnivores will match in the plot of $\delta^{13}C$ and $\delta^{15}N$
623 values corrected for trophic fractionation, which guarantees that each predator will be enclosed in a
624 triangle defined by its three main ungulate prey species (Fig. 6). The relative contributions of each
625 ungulate prey to the diet of each hypercarnivore were calculated using the software *IsoSource* v.
626 1.3.1 (**http://www.epa.gov/wed/pages/models/stableIsotopes/isosource/IsoSourceV1_3_1.zip**).

627 Obviously, there are many possible solutions for the diet of each predator, but the reasonable
628 ones (i.e., those that do not provide negative estimates for one or more prey species) involve only
629 three possible ungulate prey according to the spatial distribution of predators in the $\delta^{13}C$ - $\delta^{15}N$
630 diagram (see Phillips and Gregg, 2003: Fig. 6). It is worth noting, however, that the software
631 *IsoSource* allows estimating the dietary contributions of more than three preys. In doing so, the
632 program calculates the mean proportion for each ungulate in the diet of a given predator using the
633 average of the estimates obtained in all the combinations of three potential preys. However, this
634 procedure provides non-unique solutions, which results in increased uncertainty on the source
635 contributions (see discussions in Phillips and Gregg, 2001, 2003; Phillips et al., 2005). In addition,
636 if all ungulate species preserved in the assemblage are considered as a potential prey of each
637 carnivore, this would lead to unrealistic solutions (e.g., to consider that the wild dog *L. lycaonoides*
638 hunted megafauna or that the large sabre-tooth *H. latidens* pursued small ungulates; see discussion

639 in Palmqvist et al., 1996), which would in turn distort the estimates obtained for the more probable
640 preys.

641 The $\delta^{13}C$ - $\delta^{15}N$ plot displayed on Figure 6 shows the prey combinations for the four
642 hypercarnivores under the most realistic scenario according to previous ecomorphological studies
643 on the Venta Micena predators and their analogies to modern carnivores (Palmqvist et al., 1996,
644 2003; Palmqvist and Arribas, 2001). It is worth introducing, however, a cautionary note on the
645 reliability of the contributions of each prey to the diet of each predator, as they would vary if other
646 enrichment factors are used. According to our results (Fig. 6), the preferred preys of *H. latidens*
647 were grazing and mixed-feeding herbivores from open habitat of medium-to-large size, *Bison* sp.
648 (52%), *E. altidens* (38%) and *M. meridionalis* (10%) (Figs. 7A, C). The likelihood of such
649 specialized hunting behaviour is evident in the case of the related North American species *H.*
650 *serum,* known in high numbers from the late Pleistocene site of Friesenhahn cave, a locality
651 interpreted as a sabre-tooth's den and associated with numerous skeletal remains of adult bison and
652 juvenile mammoths (Marean and Ehrhardt, 1995). The diet of sabre-tooth *M. whitei* includes *E.*
653 *altidens* (59%), *P. verticornis* (31%) and *S. minor* (10%) (Figs. 7E, F). The jaguar *P.*
654 *gombaszoegensis* preyed upon *P. verticornis* (43%), *Pseudodama* sp. (38%) and *S. minor* (19%).
655 Finally, the pack hunting *L. lycaonoides* was likely the most versatile predator of this early
656 Pleistocene community due to its social behaviour (Palmqvist et al., 1999) and had a diet that
657 included *E. altidens* (58%), *H. albus* (30%) and *Pseudodama* sp. (12%), which are low-to-medium
658 sized ungulates from open habitat (Fig. 7D). This combination of prey species is not unreasonable
659 for *L. lycaonoides,* as modern painted dogs show similar predatory habits in the Serengeti, where
660 Thomson's gazelle and zebra represent 38% and 20% of prey captures, respectively (Malcom and
661 Van Lawick, 1975).

662 The distribution of ungulate prey described above, based on isotopic signatures, reflect
663 resource partitioning among sympatric predators in Venta Micena. According with the results
664 obtained, coursing carnivores *H. latidens* and *L. lycaonoides* hunted ungulate prey in open habitat,

665 while *M. whitei* and *P. gombaszoegensis* ambushed their prey in the margins between forest and
666 savannah. This is congruent with the palaeoenvironmental reconstruction of Venta Micena, which is
667 interpreted as a wooded savannah (Mendoza et al., 2005). It is interesting to note that the short-
668 faced hyena, *P. brevirostris,* a species specializing in scavenging the prey of hypercarnivores,
669 shows a $\delta^{15}N$ value (Fig. 3) that matches the one expected for a carnivore that consumed all of the
670 ungulates from open habitat preserved in the faunal assemblage (Fig. 7G, H).

671 Figure 8 shows the average frequencies of ungulate species estimated for a hypothetical death
672 assemblage based on the expectations of the dual linear mixing model. Such frequencies were
673 calculated assuming that: 1) each carnivore exploited the carcasses of its prey to the same degree;
674 and 2) that each predator contributed similar proportions of kills to the death assemblage collected
675 by the hyenas. This theoretical assemblage was compared with the relative frequencies of
676 herbivores in Venta Micena, based on *NISP* counts after correction for preservational bias related to
677 body size (Arribas and Palmqvist, 1998). In general terms, there are only relatively minor
678 differences between the expected and observed abundance for most ungulate species. This suggests
679 that the hyenas scavenged the ungulate carcasses in the proportions in which they were available
680 and confirms the accuracy of the estimates obtained with the mixing model on the diet of the Venta
681 Micena predators.

682 **6. Conclusions**

683 Patterns of abundance of stable-isotopes of bone collagen ($\delta^{13}C$, $\delta^{15}N$) and bioapatite ($\delta^{18}O$)
684 are a useful proxy for reconstructing the trophic structure of the early Pleistocene large mammal
685 community preserved at Venta Micena, and help also in deciphering the relationships between
686 predators and their potential prey. Carbon-isotope ratios reveal physiologic differences between
687 hindgut and foregut fermenting ungulates related to their digestive systems and the differential
688 assimilation of cellulose, with perissodactyls showing a lower isotopic enrichment than elephants
689 and artiodactyls from open habitat. The low values seen in cervids suggest that they were mixed
690 feeders or browsers in closed habitat. Nitrogen-isotope ratios of carnivore and herbivore species

691 reflect the isotopic enrichment expected from increasing one trophic level, indicating that the
692 collagen preserved was not diagenetically altered. All ungulate species except the hippo and the
693 muskoxen record isotopic values that agree with a diet of $N_2$-fixing plants. Cervids show depleted
694 $\delta^{15}N$ values resulting from soil acidity in forest, which confirm a browsing diet in closed habitat.
695 The high nitrogen ratio of *H. antiquus* suggests that this species fed predominantly on aquatic
696 vegetation. In the case of *Praeovibos* sp., this mountainous species probably fed on lichens.
697 Oxygen-isotopes of enamel and bone apatite reveal that fallow deer *Pseudodama* and bovids
698 *Hemitragus* and *Soergelia* derived most of their water requirements from the vegetation rather than
699 from drinking. The low $\delta^{18}O$ values of megacerine deer *Praemegaceros* and of megaherbivores
700 *Stephanorhinus, Hippopotamus* and *Mammuthus* suggest a greater degree of water dependence for
701 these species.

702 Carbon- and nitrogen-isotope ratios in carnivores reflect resource partitioning among
703 sympatric predators, providing interesting clues on predator-prey relationships within this ancient
704 community. The application of the dual linear mixing model allows estimating quantitatively the
705 contribution of several ungulate preys to the diet of each hypercarnivore. Specifically, the scimitar-
706 cat *Homotherium,* a coursing predator, focused on herbivores from open habitat of relatively large
707 size. The diet of *Megantereon* and the European jaguar, *P. gombaszoegensis,* included browsing
708 herbivores from closed habitat such as deer, although horses seem to have been the main prey of the
709 ambushing sabre-tooth. The pack-hunting canid *Lycaon* consumed grazing ungulates from open
710 habitat such as goat and horse. Finally, carbon- and nitrogen-isotopes of the short-faced hyena
711 *Pachycrocuta* match the values expected for a carnivore that scavenged all of the ungulates
712 preserved in the faunal assemblage, especially those that lived in open environments.

713 **Acknowledgments**

714 K. Fox-Dobbs, M.J. Kohn, B. Martínez-Navarro, J. McDonald, C. Nedin, C. Trueman, S.L.
715 Wing and an anonymous reviewer provided insightful comments on an earlier version of the
716 manuscript. Funding and analytical facilities for biogeochemical analyses were provided by the

University of Málaga, Royal Holloway University of London and at the Stable-Isotope Biogeochemistry Laboratory at McMaster University.

## References


Ambrose, S.H., DeNiro, M.J. 1986. The isotopic ecology of East African mammals. Oecologia 69, 395–406.

Anadón, P., Julià, R. 1990. Hydrochemistry from Sr and Mg contents of ostracodes in Pleistocene lacustrine deposits, Baza Basin (SE Spain). Hydrobiologia 197, 291–303.

Anadón, P., Utrilla, R., Julià, R. 1994. Palaeoenvironmental reconstruction of a Pleistocene lacustrine sequence from faunal assemblages and ostracode shell geochemistry, Baza Basin, SE Spain. Palaeogeography, Palaeoclimatology, Palaeoecology 111, 191–205.

Andrews, P., Lord, J., Nesbit-Evans, E.M. 1979. Patterns of ecological diversity in fossil and modern mammalian faunas. Biological Journal of the Linnean Society 11, 177–205.

Anyonge, W. 1996. Locomotor behaviour in Plio-Pleistocene sabre-tooth cats: a biomechanical analysis. Journal of Zoology 238, 395–413.

Arribas, A., Palmqvist, P. 1998. Taphonomy and palaeoecology of an assemblage of large mammals: hyaenid activity in the lower Pleistocene site at Venta Micena (Orce, Guadix-Baza Basin, Granada, Spain). Geobios 31 (suppl.), 3–47.

Arribas, A., Palmqvist, P. 1999. On the ecological connection between sabre-tooths and hominids: faunal dispersal events in the lower Pleistocene and a review of the evidence for the first human arrival in Europe. Journal of Archaeological Science 26, 571–585.

Ayliffe, L.K., Lister, A.M., Chivas, A.R. 1992. The preservation of glacial-interglacial climatic signatures in the oxygen isotopes of elephant skeletal phosphate: Palaeogeography, Palaeoclimatology, Palaeoecology 99, 179–191.

740 Barboza, P.S., Reynolds, P.R. 2004. Monitoring nutrition of a large grazer: muskoxen on the Arctic
741 Refuge. International Congress Series 1275, 327– 333.

742 Bell, R.H.V. 1971. A grazing ecosystem in the Serengeti. Scientific American 225, 86–93.

743 Biknevicius, A.R., Van Valkenburgh, B. 1996. Design for killing: craniodental adaptations of
744 predators. In: Gittleman, J.L. (Ed.), Carnivore Behavior, Ecology, and Evolution, Vol. 2. Cornell
745 University Press, Ithaca, NY, pp. 393–428.

746 Bocherens, H., Drucker, D. 2003. Trophic level isotopic enrichment of carbon and nitrogen in bone
747 collagen: case studies from recent and ancient terrestrial ecosystems. International Journal of
748 Osteoarchaeology 13, 46–53.

749 Bocherens, H., Billiou, D., Patou-Mathis, M., Otte, M., Bonjean, D., Toussaint, M., Mariotti, A.
750 1999. Palaeoenvironmental and palaeodietary implications of isotopic biogeochemistry of late
751 interglacial Neanderthal and mammal bones in Scladina Cave (Belgium). Journal of
752 Archaeological Science 26, 599–607.

753 Bocherens, H., Billiou, D., Mariotti, A., Toussaint, M., Patou-Mathis, M., Bonjean, D., Otte, M.
754 2001. New isotopic evidence for dietary habits of Neanderthals from Belgium. Journal of Human
755 Evolution 40, 497–505.

756 Bocherens, H., Fogel, M.L., Tuross, N., Zeder, M. 1995. Trophic structure and climatic information
757 from isotopic signatures in Pleistocene cave fauna of Southern England. Journal of
758 Archaeological Science 22, 327–340.

759 Bocherens, H., Koch, P.L., Mariotti, A., Geraads, D., Jaeger, J.J. 1996a. Isotopic biogeochemistry
760 ($^{13}C$, $^{18}O$) and mammalian enamel from African Pleistocene hominid sites. Palaios 11, 306–318.

761 Bocherens, H., Pacaud, G., Petr, A., Lazarev, P.A., Mariotti, A. 1996b. Stable isotope abundances
762 ($^{13}C$, $^{15}N$) in collagen and soft tissues from Pleistocene mammals from Yakutia: implications for
763 the palaeobiology of the mammoth steppe. Palaeogeography, Palaeoclimatology, Palaeoecology
764 126, 31–44.

765 Bocherens, H., Drucker D.G., Billiou, D., Patou-Mathis, M., Vandermeersch, B. 2005. Isotopic
766 evidence for diet and subsistence pattern of the Saint-Césaire I Neanderthal: review and use of a
767 multi-source mixing model. Journal of Human Evolution 49, 71–87.

768 Boisserie, J.R., Zazzo, A., Merceron, G., Blondel, C., Vignaud, P., Likius, A., Taïsso-Mackaye, H.,
769 Brunet, M. 2005. Diets of modern and late Miocene hippopotamids: evidence from carbon
770 isotope composition and micro-wear of tooth enamel. Palaeogeography, Palaeoclimatology,
771 Palaeoecology 221, 153–174.

772 Bryant, J.D., Froelich, P.N. 1995. A model of oxygen isotope fractionation in body water of large
773 mammals. Geochimica et Cosmochimica Acta 59, 4523–4537.

774 Bryant, J.D., Koch, P.L., Froelich, P.N., Showers, W.J., Genna, B.J. 1996. Oxygen isotope
775 partitioning between phosphate and carbonate in mammalian apatite. Geochimica et
776 Cosmochimica Acta 60, 5145–5148.

777 Cerling, T.E., Harris, J.M. 1999. Carbon isotope fractionation between diet and bioapatite in
778 ungulate mammals and implications for ecological and paleoecological studies. Oecologia 120,
779 347–63.

780 Cerling, T.E., Harris, J.M., Leakey, M.G. 1999. Browsing and grazing in elephants: the isotope
781 record of modern and fossil proboscideans. Oecologia 120, 364–374.

782 Cerling, T.E., Harris, J.M., Passey, B.H. 2003. Diets of east African bovidae based on stable isotope
783 analysis. Journal of Mammalogy 84, 456–470.

784 Chivas, A.R., De Deckker, P., Shelley, J.M.G. 1985. Strontium content of ostracods indicates
785 lacustrine palaeosalinity. Nature 316, 251–253.

786 Chivas, A.R., De Deckker, P., Shelley, J.M.G. 1986. Magnesium content of non-marine ostracod
787 shells: A new palaeosalinometer and palaeothermometer. Palaeogeography, Palaeoclimatology,
788 Palaeclimatology 54, 43–61.

789 Clauss, M., Frey, R., Kiefer, B., Lechner-Doll, M., Loehlein, W., Polster, C., Rössner, G.E., Streich,
790 W.J. 2003. The maximum attainable body size of herbivorous mammals: morphophysiological
791 constraints on foregut, and adaptations of hindgut fermenters. Oecologia 136, 14–27.

792 Coltrain, J.B., Harris, J.M., Cerling, T.E., Ehleringer, J.R., Dearing, M-D., Ward, J., Allen, J. 2004.
793 Rancho La Brea stable isotope biogeochemistry and its implications for the palaeoecology of late
794 Pleistocene, coastal southern California. Palaeogeography, Palaeoclimatology, Palaeoecology
795 205, 199–219.

796 Crutzen, P. J., Aslemann, I., Seiler, W. 1986. Methane production by domestic animals, wild
797 ruminants, and other herbivorous fauna, and humans. Tellus 38B, 271–284.

798 Damuth, J. 1992. Taxon-free characterization of animal communities: *in* Behrensmeyer, A.K.,
799 Damuth, J.D., DiMichelle, W.A., Potts, R., Sues, H.D., and Wing, S.L., eds., Terrestrial
800 Ecosystems through Time: Evolutionary Paleoecology of Terrestrial Plants and Animals: The
801 University of Chicago Press, Chicago, p. 183–203.

802 DeNiro, M.J., Epstein, S. 1978. Influence of diet on the distribution of carbon isotopes in animals.
803 Geochimica et Cosmochimica Acta 42, 495–506.

804 Demment, M.W., Van Soest, P.J. 1985. A nutritional explanation for body-size patterns of ruminant
805 and nonruminant herbivores. American Naturalist 125, 641–672.

806 Drucker, D., Bocherens, H. 2004. Carbon and nitrogen stable isotopes as tracers of change in diet
807 breadth during Middle and Upper Palaeolithic in Europe. International Journal of
808 Osteoarchaeology 14, 162–177.

809 Drucker, D., Bocherens, H., Bridault, A., Billiou, D. 2003. Carbon and nitrogen isotopic
810 composition of red deer (*Cervus elaphus*) collagen as a tool for tracking palaeoenvironmental
811 change during the Late-Glacial and Early Holocene in the northern Jura (France).
812 Palaeogeography, Palaeoclimatology, Palaeoecology 195, 375–388.

813 Duncan, P., Foose, T.J., Gordon, I.J., Gakahu, C.G., Loyd, M. 1990. Comparative nutrient
814 extraction from forages by grazing bovids and equids: a test of the nutritional model of equid-
815 bovid competition and coexistence. Oecologia 84, 411–418.

816 Edwards, G., Walker, D.A. 1983. $C_3$, $C_4$: Mechanisms, and Cellular and Environmental Regulation,
817 of Photosynthesis. Blackwell Scientific Publications, Oxford.

818 Fernández-Mosquera, D., Vila-Taboada, M., Grandal-d'Anglade A. 2001. Stable isotopes ($\delta^{13}C$,
819 $\delta^{15}N$) from the cave bear (*Ursus spelaeus*): a new approach to its palaeoenvironment and
820 dormancy. Proceedings of the Royal Society of London B 268, 1159–1164.

821 Flecker, R., de Villiers, S., Ellam, R.M. 2003. Modelling the effect of evaporation on the salinity-
822 $^{87}Sr/^{86}Sr$ relationship in modern and ancient marginal-marine systems: the Mediterranean
823 Messinian Salinity Crisis. Earth and Planetary Science Letters 203, 221–233.

824 Fizet, M., Mariotti, A., Bocherens, H., Lange-Badré, B., Vandermeersch, B., Borel, J.P., Bellon, G.
825 1995. Effect of diet, physiology and climate on carbon and nitrogen isotopes of collagen in a late
826 Pleistocene anthropic paleoecosystem (France, Charente, Marillac). Journal of Archaeological
827 Science 22, 67–79.

828 Fortelius, M., Kappelman, J. 1993. The largest land mammal ever imagined. Zoological Journal of
829 the Linnean Society 107, 85–101.

830 Fortelius, M., Solounias, N. 2000. Functional characterization of ungulate molars using the
831 abrasion-attrition wear gradient: a new method for reconstructing paleodiets. American Museum
832 Novitates, 3301, 1–36.

833 Geist, V. 1974. On the relationship of social evolution and ecology in ungulates. American
834 Zoologist 14, 205–220.

835 Gröcke, D.R. 1997a. Stable-isotope studies on the collagen and hydroxylapatite components of
836 fossils: palaeoecological implications. Lethaia 30, 65–78.

837 Gröcke, D.R. 1997b. Distribution of $C_3$ and $C_4$ plants in the late Pleistocene of South Australia
838 recorded by isotope biogeochemistry of collagen in megafauna. Australian Journal of Botany 45,
839 607–617.

840 Gröcke, D.R., Bocherens, H. 1996. Isotopic investigation of an Australian island environment.
841 Comptes Rendus de l'Académie des Sciences de Paris, Serie II 322, 713–719.

842 Gröcke, D.R., Bocherens, H., Mariotti, A. 1997. Annual rainfall and nitrogen-isotope correlation in
843 macropod collagen: application as a palaeoprecipitation indicator. Earth and Planetary Science
844 Letters 153, 279–285.

845 Gröcke, D.R., Palmqvist, P., Arribas, A. 2002. Biogeochemical inferences on the Early Pleistocene
846 large mammal paleocommunity from Venta Micena (Guadix-Baza basin, southeastern Spain).
847 In: De Renzi, M. (Ed.), Current Topics in Taphonomy and Fossilization. Ayuntamiento de
848 Valencia, pp. 127–142.

849 Harris, J.M., Cerling, T.E. 2002. Dietary adaptations of extant and Neogene African suids. Journal
850 of Zoology 256, 45–54.

851 Hedges, R.E.M. 2003. On bone collagen – apatite-carbonate isotopic relationships. International
852 Journal of Osteoarchaeology 13, 66–79.

853 Hoppe, K.A. 2004. Late Pleistocene mammoth herd structure, migration patterns, and Clovis
854 hunting strategies inferred from isotopic analyses of multiple death assemblages. Paleobiology
855 30, 129–145.

856 Hoppe, K.A., Koch, P.L., Carlson, R.W., Webb, S.D. 1999. Tracking mammoths and mastodons:
857 reconstruction of migratory behavior using strontium isotope ratios. Geology 27, 439–442.

858 Hu, F.S., Ito, E., Brubaker, L.B., Anderson, P.M. 1998. Ostracode geochemical record of Holocene
859 climatic change and implications for vegetational response in the Northwestern Alaska range.
860 Quaternary Research 49, 86–95.

861 Illius, A.W., Gordon, I.J. 1992. Modelling the nutritional ecology of ungulate herbivores: evolution
862 of body size and competitive interactions. Oecologia 89, 428–434.

863 Janis, C.M. 1976. The evolutionary strategy of the Equidae and the origins of rumen and caecal
864 fermentation. Evolution 30, 757–774.

865 Janis, C.M., Ehrhardt, D. 1988. Correlation of the relative muzzle width and relative incisor width
866 with dietary preferences in ungulates. Zoological Journal of the Linnean Society 92, 267–284.

867 Janis, C.M., Gordon, I.J., Illius, A.W. 1984. Modelling equid/ruminant competition in the fossil
868 record. Historical Biology 8, 15–29.

869 Jarman, P.J. 1974. The social organization of antelope in relation to their ecology. Behaviour 48,
870 215–267.

871 Jenkins, S.G., Partridge, S.T., Stephenson, T.R., Farley, S.D., Robbins, C.T. 2001. Nitrogen and
872 carbon isotope fractionation between mothers, neonates, and nursing offspring. Oecologia 129,
873 336–341.

874 Jones, A.M., O'Connell, T.C., Young, E.D., Scott, K., Buckingham, C.M., Iacumin, P., Brasier,
875 M.D. 2001. Biogeochemical data from well preserved 200 ka collagen and skeletal remains.
876 Earth and Planetary Science Letters 193, 143–149.

877 Justice, K.E., Smith, F.A. 1992. A model of dietary fiber utilization by small mammalian
878 herbivores, with empirical results for *Neotoma.* The American Naturalist 139, 398–416.

879 Kleiber, M. 1975. The Fire of Life: An Introduction to Animal Energetics. Krieger Publishing
880 Company, NY.

881 Klein, D.R., Bay, C. 1994. Resource partitioning by mammalian herbivores in the high Arctic.
882 Oecologia 97, 439–450.

883 Koch, P.L. 1998. Isotopic reconstruction of past continental environments. Annual Review of Earth
884 and Planetary Sciences 26, 573–613.

885 Koch, P.L., Fisher, D.C., Dettman, D. 1989. Oxygen isotope variations in the tusks of extinct
886 proboscideans: a measure of season of death and seasonality. Geology 17, 515–519.

887 Koch, P.L., Heisinger, J., Moss, C., Carlson, R.W., Fogel, M.L., Behrensmeyer, A.K. 1995. Isotopic
888 tracking of the diet and home range of African elephants. Science 267, 1340–1343.

889 Koch, P.L., Hoppe, K.A., Webb, S.D. 1998. The isotopic ecology of late Pleistocene mammals in
890 North America. Part 1. Florida. Chemical Geology 152, 119–138.

891 Kohn, M.J. 1996. Predicting animal $\delta^{18}O$: accounting for diet and physiological adaptation.
892 Geochimica et Cosmochimica Acta 60, 4811–4829.

893 Kohn, M.J., Schoeninger, M.J., Valley, J.W. 1996. Herbivore tooth oxygen isotope compositions:
894 effects of diet and physiology. Geochimica et Cosmochimica Acta 60, 3889–3896.

895 Lee-Thorp, J., Van der Merwe, N.J. 1987. Carbon isotope analysis of fossil bone apatite. South
896 African Journal of Science 83, 712–715.

897 Lewis, M. E. 1997. Carnivoran paleoguilds of Africa: implications for hominid food procurement
898 strategies. Journal of Human Evolution 32, 257–288.

899 Loehlein, W., Kienzle, E., Wiesner, H., Clauss, M. 2003. Investigations on the use of chromium
900 oxide as an inert external marker in captive Asian elephants (*Elephas maximus*): passage and
901 recovery rates: *in* Fidgett, A., Clauss, M., Ganslosser, U., Hatt, J.M., Nijboer, J., eds., Zoo
902 animal nutrition, vol II: Filander, Fürth, Germany, p. 223–232.

903 MacFadden, B.J. 2000. Cainozoic mammalian herbivores from the Americas: reconstructing ancient
904 diets and terrestrial communities. Annual Review of Ecology and Systematics 31, 33–59.

905 Malcolm, J.R., Van Lawick, H. 1975. Notes on wild dogs (*Lycaon pictus*) hunting zebras.
906 Mammalia 39, 231–240.

907 Marean, C.W., Ehrhardt, C.L. 1995. Paleoanthropological and paleoecological implications of the
908 taphonomy of a sabretooth's den. Journal of Human Evolution 29, 515–547.

McNab, B.K. 1986. The influence of food habits on the energetics of eutherian mammals. Ecological Monographs 56, 1–19.

McNaughton, S.J., Georgiadis, N.J. 1986. Ecology of African grazing and browsing mammals. Annual Review of Ecology and Systematics 17, 39–65.

Mcnulty, T., Calkins, A., Ostrom, P., Gandhi, H., Gottfried, M., Martin, L., Gage, D. 2002. Stable isotope values of bone organic matter: artificial diagenesis experiments and paleoecology of Natural Trap Cave, Wyoming. Palaios 17, 36–49.

Mendoza, M., Janis, C.M., Palmqvist, P. 2002. Characterizing complex craniodental patterns related to feeding behaviour in ungulates: a multivariate approach. Journal of Zoology 258, 223–246.

Mendoza, M., Janis, C.M., Palmqvist, P., 2005. Ecological patterns in the trophic-size structure of large mammal communities: a 'taxon-free' characterization. Evolutionary Ecology Research 7, 505–530.

Metges, C., Kempe, K., Schmidt, H.L. 1990. Dependence of the carbon isotope contents of breath carbon dioxide, milk, serum and rumen fermentation products on the value of food in dairy cows. Brown Journal of Nutrition 63, 187–196.

Miller, E.K., Blum, J.D., Friedland, A.J. 1993. Determination of soil exchangeable-cation loss and weathering rates using Sr isotopes. Nature 362, 438–441.

Novak, R.M. 1999. Walker´s Mammals of the World. The Johns Hopkins University Press, Baltimore and London.

Ortiz, J.E., Torres, T., Delgado, A., Reyes, E., Llamas, J.F., Soler, V., Raya, J. 2006. Pleistocene paleoenvironmental evolution at continental middle latitude inferred from carbon and oxygen stable isotope analysis of ostracodes from the Guadix-Baza Basin (Granada, SE Spain). Palaeogeography, Palaeoclimatology, Palaeoecology 240, 536–561.

932 Ostrom, P.H., Macko, S.A., Engel, M.H., Russell, D.A. 1993. Assessment of trophic structure of
933 Cretaceous communities based on stable nitrogen isotope analysis. Geology 21, 491–494.

934 Palmqvist, P., Arribas, A. 2001. Taphonomic decoding of the paleobiological information locked in
935 a lower Pleistocene assemblage of large mammals. Paleobiology 27, 512–530.

936 Palmqvist, P., Martínez-Navarro, B., Arribas, A. 1996. Prey selection by terrestrial carnivores in a
937 lower Pleistocene paleocommunity. Paleobiology 22, 514–534.

938 Palmqvist, P., Arribas, A., Martínez-Navarro, B. 1999. Ecomorphological analysis of large canids
939 from the lower Pleistocene of southeastern Spain. Lethaia 32, 75–88.

940 Palmqvist, P., Mendoza, M., Arribas, A., Gröcke, D.R. 2002. Estimating the body mass of
941 Pleistocene canids: discussion of some methodological problems and a new 'taxon free'
942 approach. Lethaia 35, 358–360.

943 Palmqvist, P., Gröcke, D.R., Arribas, A., Fariña, R. 2003. Paleoecological reconstruction of a lower
944 Pleistocene large mammals community using biogeochemical ($\delta^{13}C$, $\delta^{15}N$, $\delta^{18}O$, Sr:Zn) and
945 ecomorphological approaches. Paleobiology 29, 204–228.

946 Parker, K.L., Barboza, P.S., Stephenson, T.R. 2005. Protein conservation in female caribou
947 (*Rangifer tarandus*): effects of decreasing diet quality during winter. Journal of Mammalogy 86,
948 610-622.

949 Parra, R. 1978. Comparison of foregut and hindgut fermentation in herbivores. In: Montgomery,
950 G.G. (Ed.), The Ecology of Arboreal Folivores. Smithsonian Institution Press, Washington, pp.
951 205–230.

952 Pérez-Barbería, F.J., Gordon, I.J. 2001. Relationships between oral morphology and feeding style in
953 the Ungulata: a phylogenetically controlled evaluation. Proceedings of the Royal Society of
954 London 268, 1021–1030.

955 Phillips, D.L. 2001. Mixing models in analyses of diet using multiple stable isotopes: a critique.
956 Oecologia 127, 166–170.

957 Phillips, D.L., Gregg, J.W. 2001. Uncertainty in source partitioning using stable isotopes. Oecologia
958 127, 171–179.

959 Phillips, D.L., Gregg, J.W. 2003. Source partitioning using stable isotopes: coping with too many
960 sources. Oecologia 136, 261–269.

961 Phillips, D.L., Koch, P.L. 2002. Incorporating concentration dependence in stable isotope mixing
962 models. Oecologia 130, 114–125.

963 Phillips, D.L., Newsome, S.D., Gregg, J.W. 2005. Combining sources in stable isotope mixing
964 models: alternative methods. Oecologia 144, 520–527.

965 Price, T.D., Connor, M., Parsen, J.D. 1985. Bone chemistry and the reconstruction of diet:
966 strontium discrimination in white-tailed deer. Journal of Archaeological Science 12, 419–442.

967 Prins, R.A., Kreulen, D.A. 1991. Comparative aspects of plant cell wall digestion in mammals. In:
968 Hoshino, S., Onodera, R., Minoto, H., Itabashi, H. (Eds.), The Rumen Ecosystem: the Microbial
969 Metabolism and its Regulation. Japan Scientific Society Press, Tokyo, pp. 109–121.

970 Reed, K.E. 1998. Using large mammal communities to examine ecological and taxonomic structure
971 and predict vegetation in extant and extinct assemblages. Paleobiology 24, 384–408.

972 Richards, M.P., Hedges, R.E.M. 2003. Variations in bone collagen $\delta^{13}C$ and $\delta^{15}N$ values of fauna
973 from Northwest Europe over the last 40000 years. Palaeogeography, Palaeoclimatology,
974 Palaeoecology 193, 261–267.

975 Richards, M.P., Pettitt, P.B., Trinkaus, E., Smith, F.H., Paunovic, M., Karavanic, I. 2000.
976 Neanderthal diet at Vindija and Neanderthal predation: the evidence from stable isotopes.
977 Proceedings of the National Academy of Sciences USA 97, 7663–7666.

978 Robinson, D. 2001. $\delta^{15}N$ as an integrator of the nitrogen cycle. Trends in Ecology and Evolution 16,
979 153–162.

980 Rodière, E., Bocherens, H., Angibault, J.M., Mariotti, A. 1996. Paticularités isotopiques de l'azote
981 chez le chevreuil (*Capreolus capreolus* L.): Implications pour les reconstitutions
982 paléoenvironnementales. Comptes Rendus de l'Académie des Sciences de Paris, Serie II 323,
983 179–185.

984 Schwarcz, H.P. 1991. Some theoretical aspects of isotope paleodiet studies. Journal of
985 Archaeological Science 18, 261–275.

986 Schwarcz, H.P., Tosha, Dupras, L., Fairgrieve, S.I. 1999. $^{15}N$ enrichment in the Sahara: in search of
987 a global relationship. Journal of Archaeological Science 26, 629–636.

988 Schwarm, A., Ortmann, S., Hofer, H., Streich, W.J., Flach, E.J., Kühne, R., Hummel, J., Castell,
989 J.C., Clauss, M. 2006. Digestion studies in captive Hippopotamidae: a group of large ungulates
990 with an unusually low metabolic rate. Journal of Animal Physiology and Animal Nutrition 90,
991 300–308.

992 Schulze, E., Lohmeyer, S., Giese, W. 1998. Determination of C-13/C-12-ratios in rumen produced
993 methane and $CO_2$ of cows, sheep and camels. Isotopes in Environmental and Health Studies 34,
994 75–79.

995 Sealy J. C., Van der Merwe, N.J., Lee Thorp, J.A., Lanham, J.L. 1987. Nitrogen isotopic ecology in
996 southern Africa: implications for environmental and dietary tracing. Geochimica et
997 Cosmochimica Acta 51, 2707–2717.

998 Shipley, L.A., Gross, J.E., Spalinger, D.E., Thompsom-Hobbs, N., Wunder, B.A. 1994. The scaling
999 of intake rate in mammalian herbivores. The American Naturalist 143, 1055–1082.

1000 Sillen, A., Lee-Thorp, J.A. 1994. Trace element and isotopic aspects of predator-prey relationships
1001 in terrestrial foodwebs. Palaeogeography, Palaeoclimatology, Palaeoecology 107, 243–255.

1002 Smith, B.N., Epstein, S. 1971. Two categories of $^{13}C/^{12}C$ ratios for higher plants. Plant Physiology
1003 47, 380–384.

1004 Soligo, C., Andrews, P. 2005. Taphonomic bias, taxonomic bias and historical non-equivalence of
1005 faunal structure in early hominin localities. Journal of Human Evolution 49, 206–229.

1006 Solounias, N., Moelleken, S.M.C. 1993. Tooth microwear and premaxillary shape of an archaic
1007 antelope. Lethaia 26, 261–268.

1008 Sponheimer, M., Lee-Thorp, J.A. 2001. The oxygen isotope composition of mammalian enamel
1009 carbonate from Morea State, South Africa. Oecologia 126, 153–157.

1010 Springer, M.S., Cleven, G.C., Madsen, O., de Jong, W.W., Waddell, V.G., Amrine, H.M.,
1011 Stanhope, M.J. 1997. Edemic African mammals shake the phylogenetic tree. Nature 388, 61–64.

1012 Szepanski, M.M., Ben-David, M., Van Ballenberghe, V. 1999. Assessment of salmon resources in
1013 the diet of the Alexander Archipelago wolf using stable isotope analysis. Oecologia 120, 327–
1014 335.

1015 Torres, J.M., Borja, C., García-Olivares, E. 2002. Immunoglobulin G in 1.6 million-year-old fossil
1016 bones from Venta Micena (Granada, Spain): Journal of Archaeological Science 29, 167–175.

1017 Turner, A., Antón, M. 1996. The giant hyaena, *Pachycrocuta brevirostris* (Mammalia, Carnivora,
1018 Hyaenidae). Geobios 29, 455–468.

1019 Van der Merwe, N.J. 1989. Natural variation in $^{13}C$ concentration and its effect on environmental
1020 reconstruction using $^{13}C/^{12}C$ ratios in animal bones: *in* Pride, T.D., ed., The chemistry of
1021 prehistoric human bone: Cambridge University Press, Cambridge, p. 105–125.

1022 Van Soest, P.J. 1994. Nutritional ecology of the ruminant, 2nd edn: Cornell University Press,
1023 Ithaca, 476 p.

1024 Van Soest, P.J. 1996. Allometry and ecology of feeding behavior and digestive capacity in
1025 herbivores: a review: Zoo Biology, v. 15, p. 455–479

1026 Van Valkenburgh, B. 1985. Locomotor diversity within past and present guilds of large predatory
1027 mammals: Paleobiology, v. 11, p. 406–428.

1028 Van Valkenburgh, B. 1988. Trophic diversity in past and present guilds of large predatory
1029 mammals: Paleobiology, v. 14, p. 155–173.

1030 Vanderklift, M.A., Ponsard, S. 2003. Sources of variation in consumer-diet $\delta^{15}N$ enrichment: a
1031 meta-analysis. Oecologia, v. 136, p. 169–182.

1032 Vermorel, M., Martin-Rosset, W., Vernet, J. 1997. Energy utilization of twelve forages or mixed
1033 diets for maintenance by sport horses: Science, v. 47, p. 157–167.

1034 Virginia, R.A., Jarrell, W.M., Rundel, P.W., Shearer, G., Kohl, D.H. 1989. The use of variation in
1035 the natural abundance of $^{15}N$ to assess symbiotic nitrogen fixation by woody plants: *in* Rundel,
1036 P.W., Ehleringer, J.R., Nagy, K.A., eds., Stable Isotopes in Ecological Research: Springer-
1037 Verlag, New York, p. 345–394.

1038 Williams, S.H., and Kay, R.F. 2001, A comparative test for adaptive explanations for hypsodonty in
1039 ungulates and rodents: Journal of Mammalian Evolution, v. 8, p. 207–229.

1040 Wing, S.L., Sues, H.D., Potts, R., DiMichelle, W.A., and Behrensmeyer, A.K. 1992,. Evolutionary
1041 paleoecology: *in* Behrensmeyer, A.K., Damuth, J.D., DiMichelle, W.A., Potts, R., Sues, H.D.,
1042 and Wing, S.L., eds., Terrestrial Ecosystems through Time: Evolutionary Paleoecology of
1043 Terrestrial Plants and Animals: The University of Chicago Press, Chicago, p. 1–13.

1044

1045 **Figure 1.** A: average values of trace-elements (Fe, Mg, Na, Mn, and Sr, in ppm), and B: bulk rock
1046 stable-isotope ratios ($\delta^{13}C$ and $\delta^{18}O$, in ‰, $^{87}Sr/^{86}Sr$) in the samples of sediment collected from
1047 the stratigraphic column of the early Pleistocene locality of Venta Micena. C: reconstruction of
1048 paleoenvironmental changes in the lake at Venta Micena during early Pleistocene times, inferred
1049 from the abundance of trace elements and bulk-rock $\delta^{18}O$ analyses in samples collected through
1050 the Venta Micena stratigraphic section.

1051

1052 **Figure 2.** Plot of $\delta^{13}C$ and $\delta^{15}N$ values of collagen material extracted from bone samples of large
1053 mammal species preserved in the lower Pleistocene site of Venta Micena (data from Table 2).
1054 The lines represent one standard deviation around the mean for those species in which at least
1055 two measurements of stable-isotopes were available.

1056

1057 **Figure 3.** Box diagrams of $\delta^{13}C$ and $\delta^{15}N$ values of collagen material extracted from bone samples
1058 of large mammal species preserved in Venta Micena (data from Table 2).

1059

1060 **Figure 4.** Box diagrams of $\delta^{18}O$ values of hydroxylapatite from bone samples and tooth enamel of
1061 large mammal species preserved in Venta Micena (data from Table 2).

1062

1063 **Figure 5.** Histograms showing the distribution of mean values of isotopic enrichment of carbon-
1064 and nitrogen-isotopes ($\Delta\delta^{13}C$ and $\Delta\delta^{15}N$, respectively) in bone collagen between mammalian
1065 carnivores and their potential prey for several living communities and fossil assemblages.
1066 Arrows indicate the values for Venta Micena (VM), obtained averaging the species means
1067 according to NISP values (*H. antiquus* and *Praeovibos* sp. excluded). Fossil assemblages (late
1068 Pleistocene to Holocene): Bocherens et al., 1995 (Kent's Cave, England); Fizet et al., 1995

(Marillac, France); Bocherens et al., 1996 (Yakutia, Russia); Gröcke 1997a (Henschke Cave, Australia); Bocherens et al., 1999 (Scladina Cave, Level 4, Belgium); Bocherens et al., 2001 (Scladina Cave, Levels 1A-1B, Belgium); McNulty et al., 2002 (Natural Trap Cave, USA); Bocherens and Drucker, 2003 (Saint Germain – la Rivière, France; Les Jamblancs, France); Coltrain et al., 2004 (Rancho La Brea, USA); Drucker and Bocherens, 2004 (Saint Césaire – Camiac – La Berbie, France). Recent communities: Ambrose and DeNiro, 1986 (East Africa); Sealy et al., 1987 (Kasungu National Park, Malawi); Van der Merwe, 1989 (South Africa); Schwarcz, 1991 (Ontario, Canada); Sillen and Lee-Thorp, 1994 (Southwestern Cape, South Africa); Bocherens et al., 1996b (Yakutia, Russia); Szepanski et al., 1999 (Alaska, USA); Bocherens and Drucker, 2003 (Bielowiecza forest, Poland).

**Figure 6.** Plot of $\delta^{13}C$ and $\delta^{15}N$ values for carnivore and ungulate species from Venta Micena, corrected for trophic fractionation ($\Delta\delta^{13}C$ = 0.8‰, $\Delta\delta^{15}N$ = 2.8‰). Each of the four hypercarnivore species lies within the triangle defined by its three most probable prey species. According to the linear mixing model (Phillips, 2001), the contribution to carnivore diet of each prey defining a vertex in the triangle is obtained as the distance from this vertex to the opposed side in relation to its distance to the predator (both measured on the line connecting prey and predator). Black circles: ungulates; white circles: hypercarnivores; gray circles: omnivores and bone-cracking hyena.

**Figure 7.** Reconstruction of the predatory behaviour of the early Pleistocene hypercarnivores preserved in Venta Micena, according to biogeochemical and ecomorphological inferences. Machairodont *Homotherium latidens,* a pursuit predator, hunted subadult elephants (A) and juveniles of other megaherbivore species such as hippo (B), but these prey represented a minor fraction of its diet, which predominantly included ungulates of medium-to-large size from open environment such as bison (C) and horse. Saber-tooth *Megantereon whitei,* an ambusher, hunted

ungulates from open habitat such as horse (D) and browsing deer from forest (E). The hypercarnivorous canid *Lycaon lycaonoides* probably had a pack-hunting behaviour similar to that of modern African painted dogs, with small-to-medium sized ungulates such as goat as their main prey (F). The giant hyena, *Pachycrocuta brevirostris,* scavenged ungulate carcasses left by the hypercarnivores (G) and transported skeletal elements to the denning site (H), a conclusion also supported by taphonomic evidence (Palmqvist et al., 1996; Arribas and Palmqvist, 1998; Palmqvist and Arribas, 2001). Drawings by Mauricio Antón.

.

**Figure 8.** Comparison between the relative abundance of ungulates in the large mammals assemblage from Venta Micena, corrected for taphonomic bias resulting from differences in body mass (Arribas and Palmqvist, 1998), and the relative frequencies in which these species were hunted by the four hypercarnivores, deduced in this article from the application of the linear mixing model and assuming that each predator contributed similarly to the kill assemblage collected by the hyenas.

1110 **Table 1**. Height (m), trace-element abundance (ppm) and bulk-rock stable-isotope ratios
1111 ($\delta^{13}C$, $\delta^{18}O$, in ‰; $^{87}Sr/^{86}Sr$) of sedimentary samples (vm-1 to vm-10) collected through the
1112 stratigraphic section of Venta Micena.

1113

| sample | height | Fe | Mg | Na | Mn | Sr | Ca | $\delta^{13}C$ | $\delta^{18}O$ | $^{87}Sr/^{86}Sr$ |
|---|---|---|---|---|---|---|---|---|---|---|
| vm-11 | 3.85 | 897 | 3975 | 500 | 40 | 979 | 303917 | -7.36 | -5.57 | 0.707836 |
| vm-10 | 3.35 | 2143 | 5556 | 682 | 22 | 1197 | 279964 | -6.98 | -5.40 | 0.707857 |
| vm-9 | 3.15 | 1007 | 6068 | 3245 | 40 | 831 | 297197 | -7.42 | -5.75 | 0.707826 |
| vm-8 | 2.50 | 2486 | 6202 | 334 | 50 | 327 | 195090 | -5.19 | -5.18 | 0.708020 |
| vm-7 | 1.95 | 1695 | 7396 | 438 | 107 | 435 | 256736 | -5.60 | -4.80 | 0.707972 |
| vm-6 | 1.65 | 2526 | 8101 | 389 | 105 | 414 | 236984 | -5.23 | -5.18 | 0.707990 |
| vm-5 | 1.40 | 4551 | 8146 | 554 | 120 | 447 | 224936 | -5.31 | -4.93 | 0.707989 |
| vm-4 | 1.15 | 2256 | 6465 | 430 | 93 | 449 | 260913 | -5.61 | -5.37 | 0.707947 |
| vm-3 | 1.05 | 5366 | 8768 | 754 | 95 | 555 | 202355 | -5.53 | -4.31 | 0.708008 |
| vm-2 | 0.85 | 4401 | 17445 | 1019 | 48 | 647 | 137997 | -6.34 | -4.59 | 0.707891 |
| vm-1 | 0.40 | 4400 | 68451 | 1656 | 136 | 313 | 126781 | -4.12 | 1.79 | 0.707949 |

1114
1115

1116 **Table 2.** C:N proportions and isotopic ratios from collagen ($\delta^{13}C$, $\delta^{15}N$) and hydroxylapatite ($\delta^{18}O$)
1117 extracted from bone and tooth samples of large mammal species preserved in the early
1118 Pleistocene locality of Venta Micena (juv.: juvenile, subad.: subadult; ad.: adult).

| Species | Sample code | Fossil specimen (tooth or bone portion) | $\delta^{13}C_{col.}$ | $\delta^{15}N_{col.}$ | $\delta^{18}O_{hyd.}$ | $C:N_{col.}$ |
|---|---|---|---|---|---|---|
| *Mammuthus meridionalis* (juv.) | VM-4439 | proximal metacarpal | -21,4 | +4,7 | -4,5 | 3,1 |
| *Mammuthus meridionalis* (juv.) | VM-OX1 | enamel fragment of deciduous tooth | -- | -- | -3,9 | -- |
| *Mammuthus meridionalis* (juv./subad.) | VM-3581 | vertebrae fragment (neural arch) | -20,6 | +2,9 | -2,8 | 3,3 |
| *Mammuthus meridionalis* (juv./subad.) | VM-3581b | vertebrae fragment (neural arch) | -23,4 | +4,3 | -5,3 | 3,6 |
| *Mammuthus meridionalis* (subad./ad.) | VM-2172 | carpal bone | -21,1 | +3,2 | -5,9 | 3,4 |
| *Mammuthus meridionalis* (subad./ad.) | VM-4482 | carpal bone | -- | -- | -4,7 | -- |
| *Mammuthus meridionalis* (juv.) | VM-4607 | cranial fragment of a newborn individual or fetus | -22,8 | +3,5 | -4,5 | 3,5 |
| *Mammuthus meridionalis* (juv.) | VM-4607b | cranial fragment of a newborn individual or fetus | -22,9 | +3,2 | -4,5 | 3,2 |
| *Mammuthus meridionalis* (juv.) | VM-84-C3-C8-49 | left maxilla with $dP^2$ and $dP^3$ partially worn | -- | -- | -4,5 | -- |
| *Mammuthus meridionalis* (juv.) | VM-4439b | proximal metacarpal | -23,4 | +3,8 | -5,3 | 3,2 |
| *Mammuthus meridionalis* (juv.) | VM-3674 | vertebrae fragment | -- | -- | -5,0 | -- |
| cf. *Mammuthus meridionalis* (juv.) | VM-4332 | right humeral diaphysis of a newborn individual | -- | -- | -1,4 | -- |
| cf. *Mammuthus meridionalis* (juv.) | VM-1919 | left humeral diaphysis of a newborn individual | -22,2 | +5,1 | -5,6 | 3,6 |
| Mean for *Mammuthus* (N = 8/13) | | | -22,23 $\pm$ 1,08 | +3,84 $\pm$ 0,79 | -4,45 $\pm$ 1,21 | 3,36 $\pm$ 0,1 |
| *Hippopotamus antiquus* (ad.) | VM-4123 | right fifth metacarpal | -22,3 | +7,7 | -2,1 | 3,5 |
| *Hippopotamus antiquus* (ad.) | VM-OX6 | enamel fragment of permanent tooth | -- | -- | -5,8 | 3,4 |
| *Hippopotamus antiquus* (ad.) | VM-4299 | left proximal humerus | -22,6 | +7,4 | -3,7 | 3,4 |
| *Hippopotamus antiquus* (ad.) | VM-3680 | left femur | -21,2 | +7,1 | -5,8 | 3,5 |
| *Hippopotamus antiquus* (juv.) | VM-3558 | right femur | -- | -- | -6,2 | -- |
| *Hippopotamus antiquus* (juv.) | VM-3337 | left femur | -23,0 | +5,7 | -7,3 | 3,4 |
| *Hippopotamus antiquus* (juv.) | VM-84-C1-V5-13 | fragment of left mandible with unworn $dP_3$ and $dP_4$ | -22,2 | +6,0 | -7,6 | 3,2 |
| Mean for *Hippopotamus* (N = 5/7) | | | -22,26 $\pm$ 0,67 | +6,78 $\pm$ 0,88 | -5,50 $\pm$ 1,96 | 3,40 $\pm$ 0,1 |
| *Bison* sp. (ad.) | VM-3473 | right proximal metacarpal | -22,1 | +3,8 | -2,2 | 3,1 |
| *Bison* sp. (ad.) | VM-3503 | distal metatarsal | -21,5 | +3,6 | -4,1 | 3,3 |
| *Bison* sp. (ad.) | VM-4185 | left proximal metacarpal | -- | -- | -2,8 | -- |
| *Bison* sp. (ad.) | VM-4444 | left proximal metatarsal | -- | -- | -3,1 | -- |
| *Bison* sp. (ad.) | VM-OX7 | enamel fragment of permanent tooth | -- | -- | -5,2 | -- |
| *Bison* sp. (ad.) | VM-3583 | left distal humerus | -- | -- | -3,7 | -- |
| *Bison* sp. (ad.) | VM-3473b | right proximal metacarpal | -21,4 | +3,5 | -3,2 | 3,3 |
| *Bison* sp. (ad.) | VM-544 | left distal humerus | -21,8 | +4,0 | -4,3 | 3,4 |
| *Bison* sp. (ad.) | VM-4164 | left distal humerus | -- | -- | -3,3 | -- |
| *Bison* sp. (juv.) | VM-4378 | right mandible with $dP_2$-$dP_4$ and unworn $M_1$ | -22,7 | +4,6 | -3,5 | 3,5 |
| *Bison* sp. (juv./subad.) | VM-non coded | right maxilla, with unworn $P^2$-$P^4$ and $M^1$ | -22,4 | +3,1 | -4,8 | 3,6 |
| Mean for *Bison* (N = 6/11) | | | -21,98 $\pm$ 0,51 | +3,77 $\pm$ 0,51 | -3,85 $\pm$ 1,08 | 3,37 $\pm$ 0,1 |
| *Praeovibos* sp. (ad.) | VM-1742 | left metacarpal with fused epiphyses | -22,0 | +6,7 | -4,7 | 3,2 |
| *Soergelia minor* (ad.) | VM-3448 | right distal tibia | -- | -- | -2,7 | -- |

| | | | | | | |
|---|---|---|---|---|---|---|
| *Soergelia minor* (ad.) | VM-3867 | left metatarsal | -23,2 | +3,2 | -2,1 | 3,4 |
| *Soergelia minor* (ad.) | VM-3867b | left metatarsal | -23,5 | +3,4 | -2,3 | 3,5 |
| *Soergelia minor* (ad.) | VM-OX10 | enamel fragment of permanent tooth | -- | -- | -2,6 | -- |
| *Soergelia minor* (ad.) | VM-3982 | left proximal metatarsal | -23,0 | +3,8 | -2,7 | 3,3 |
| *Soergelia minor* (subad.) | VM-4597 | maxilla with unworn $P^2$-$P^4$ and $M^1$, $M^2$-$M^3$ erupting | -23,9 | +2,2 | -- | 3,6 |
| *Soergelia minor* (ad.) | VM-4336 | right horn base | -23,4 | +4,3 | -2,3 | 3,2 |
| Mean for *Soergelia* (N = 5/5) | | | -23,40 ± 0,34 | +3,38 ± 0,78 | -3,16 ± 1,88 | 3,40 ± 0,1 |
| *Hemitragus albus* (ad.) | VM-3802 | left distal metatarsal | -20,9 | +4,0 | -3,4 | 3,3 |
| *Hemitragus albus* (ad.) | VM-3922 | right distal metacarpal | -20,1 | +3,9 | -1,5 | 3,4 |
| *Hemitragus albus* (ad.) | VM-OX11 | enamel fragment of permanent tooth | -- | -- | -3,3 | -- |
| *Hemitragus albus* (ad.) | VM-3157 | distal metatarsal | -- | -- | -2,1 | -- |
| *Hemitragus albus* (ad.) | VM-3449 | left distal humerus | -20,4 | +3,7 | -2,9 | 3,5 |
| *Hemitragus albus* (ad.) | VM-4541a | distal right humerus with fused epiphysis | -21,6 | +3,4 | -3,6 | 3,6 |
| Mean for *Hemitragus* (N = 4/6) | | | -20,75 ± 0,66 | +3,75 ± 0,26 | -2,80 ± 0,83 | 3,45 ± 0,1 |
| *Pseudodama* sp. (ad.) | VM-3055 | right proximal metatarsal | -- | -- | -3,2 | -- |
| *Pseudodama* sp. (ad.) | VM-3482 | left proximal metacarpal | -23,6 | +2,5 | -2,6 | 3,5 |
| *Pseudodama* sp. (ad.) | VM-4330 | left proximal metacarpal | -- | - | -2,4 | -- |
| *Pseudodama* sp. (ad.) | VM-OX9 | enamel fragment of permanent tooth | -- | -- | -2,6 | -- |
| *Pseudodama* sp. (ad.) | VM-4410 | fragment of left hemimandible with $M_1$-$M_3$ | -- | -- | -2,9 | -- |
| *Pseudodama* sp. (ad.) | VM-3047 | right distal metacarpal | -23,8 | +2,9 | -3,0 | 3,3 |
| *Pseudodama* sp. (ad.) | VM-3060 | right proximal metacarpal | -23,2 | +2,6 | -2,5 | 3,4 |
| *Pseudodama* sp. (subad.) | VM-4409 | left mandible with $dP_4$ heavily worn and $M_1$ | -22,8 | +1,8 | -2,8 | 3,2 |
| *Pseudodama* sp. (subad.) | VM-4037 | right mandible with $dP_3$-$dP_4$ and $M_1$ slightly worn | -22,2 | +2,2 | -1,3 | 3,0 |
| Mean for *Pseudodama* (N = 5/9) | | | -23,12 ± 0,64 | +2,40 ± 0,42 | -2,59 ± 0,55 | 3,28 ± 0,1 |
| *Praemegaceros verticornis* ad.) | VM-3297 | fragment of right metacarpal diaphysis | -25,9 | +1,6 | -3,3 | 3,2 |
| *Praemegaceros verticornis* (ad.) | VM-4155 | left proximal radius | -- | -- | -2,8 | -- |
| *Praemegaceros verticornis* (ad.) | VM-3111 | distal metacarpal | -- | -- | -4,0 | -- |
| *Praemegaceros verticornis* (ad.) | VM-3556 | right distal humerus | -25,6 | +1,3 | -4,2 | 3,6 |
| *Praemegaceros verticornis* (ad.) | VM-OX8 | enamel fragment of permanent tooth | -- | -- | -4,6 | -- |
| *Praemegaceros verticornis* (ad.) | VM-4181 | left distal humerus | -25,4 | +1,8 | -3,7 | 3,4 |
| *Praemegaceros verticornis* (ad.) | VM-3111b | distal metacarpal | -- | -- | -3,9 | -- |
| *Praemegaceros verticornis* (ad.) | VM-3224 | left distal metatarsal | -25,8 | +1,4 | -3,1 | 3,5 |
| *Praemegaceros verticornis* (ad.) | VM-3780 | left distal humerus | -- | -- | -4,0 | -- |
| *Praemegaceros verticornis* (juv.) | VM-84C3-E10-63 | left mandible with $dP_2$-$dP_4$ | -25,9 | +2,3 | -3,5 | 3,4 |
| *Praemegaceros verticornis* (juv.) | VM-82-9 | left maxilla with $dP^2$, $dP^3$ and $dP^4$ | -24,4 | +1,7 | -- | 3,3 |
| *Praemegaceros verticornis* (juv.) | VM-4039 | right mandible with $dP_4$ and $M_1$ erupting | -25,2 | +2,0 | -3,7 | 3,6 |
| *Praemegaceros verticornis* (juv.) | VM-4394 | fragment of right maxilla, with $dP^2$, $dP^3$, $dP^4$ and $M^1$ | -- | -- | -2,0 | -- |
| Mean for *Praemegaceros* (N = 7/12) | | | -25,46 ± 0,53 | +1,73 ± 0,35 | -3,80 ± 1,07 | 3,43 ± 0,1 |
| *Stephanorhinus etruscus* (ad.) | VM-4487 | left proximal ulna | -26,5 | +3,9 | -3,7 | 3,5 |
| *Stephanorhinus etruscus* (ad.) | VM-4510 | right humeral diaphysis | -26,6 | +3,7 | -3,7 | 3,3 |
| *Stephanorhinus etruscus* (ad.) | VM-OX4 | tooth fragment | -- | -- | -3,7 | -- |
| *Stephanorhinus etruscus* (ad.) | VM-OX5 | enamel fragment of permanent tooth | -- | -- | -5,1 | -- |
| *Stephanorhinus etruscus* (ad.) | VM-3616 | right distal femur | -26,2 | +3,5 | -4,2 | 3,3 |
| *Stephanorhinus etruscus* (ad.) | VM-3578 | left scapula | -- | -- | -4,6 | -- |
| *Stephanorhinus etruscus* (ad.) | VM-3578b | left scapula | -- | -- | -4,8 | -- |
| *Stephanorhinus etruscus* (ad.) | VM-3578c | left scapula | -25,8 | +3,0 | -5,2 | 3,2 |
| *Stephanorhinus etruscus* (ad.) | VM-3744 | right femoral diaphysis | -24,7 | -- | -4,3 | 3,1 |
| *Stephanorhinus etruscus* (juv./subad.) | VM-1908 | right distal radius with the epiphysis unfused | -25,2 | +3,6 | -4,8 | 3,6 |

| | | | | | | |
|---|---|---|---|---|---|---|
| *Stephanorhinus etruscus* (juv.) | VM-non coded | fragment of left maxilla, with $dP^2$ and $dP^3$ | -- | -- | -3,9 | -- |
| Mean for *Stephanorhinus* (N = 6/11) | | | -25,83 ± 0,76 | +3,22 ± 0,85 | -4,36 ± 0,57 | 3,33 ± 0,1 |
| *Equus altidens* (ad.) | VM-3028 | right metatarsal lacking the distal epiphysis | -26,1 | +2,0 | -2,5 | 3,2 |
| *Equus altidens* (ad.) | VM-3119 | right scapula | -26,7 | +3,5 | -2,8 | 3,6 |
| *Equus altidens* (ad.) | VM-3162 | right distal tibia | -26,0 | +3,0 | -3,0 | 3,5 |
| *Equus altidens* (ad.) | VM-3258 | right distal tibia | -- | -- | -2,9 | -- |
| *Equus altidens* (ad.) | VM-3430 | left distal metatarsal | -- | -- | -2,3 | -- |
| *Equus altidens* (ad.) | VM-3529 | left proximal scapula | -26,0 | +3,3 | -3,3 | 3,4 |
| *Equus altidens* (ad.) | VM-4189 | fragment of metatarsal diaphysis | -25,5 | +3,5 | -2,3 | 3,5 |
| *Equus altidens* (ad.) | VM-4421 | left proximal radius | -25,0 | +2,1 | -3,8 | 3,4 |
| *Equus altidens* (ad.) | VM-OX2 | enamel fragment of permanent tooth | -- | -- | -3,4 | -- |
| *Equus altidens* (ad.) | VM-OX3 | enamel fragment of permanent tooth | -- | -- | -5,2 | -- |
| *Equus altidens* (ad.) | VM-3089 | left distal metacarpal | -- | -- | -3,5 | -- |
| *Equus altidens* (ad.) | VM-4421b | left proximal radius | -25,8 | +2,8 | -3,9 | 3,4 |
| *Equus altidens* (ad.) | VM-3279 | left tibia diaphysis | -26,6 | +3,1 | -4,3 | 3,5 |
| *Equus altidens* (ad.) | VM-3428 | distal diaphysis of metatarsal | -- | -- | -2,8 | -- |
| *Equus altidens* (juv./subad.) | VM-4403 | maxilla with worn $dP^1$-$dP^4$, $M^1$-$M^3$ erupting | -25,8 | +3,5 | -2,5 | 3,6 |
| *Equus altidens* (juv.) | VM-602 | metacarpal with the proximal epiphysis unfused | -26,3 | +2,0 | -3,7 | 3,1 |
| *Equus altidens* (juv.) | VM-2073 | right metacarpal, two thirds of proximal diaphysis | -- | -- | -4,3 | -- |
| *Equus altidens* (juv.) | VM-3388 | right mandible fragment, with unworn $dP_2$-$dP_4$ | -25,1 | +2,6 | -5,2 | 3,5 |
| Mean for *Equus* (N = 11/18) | | | -25,90 ± 0,55 | +2,85 ± 0,60 | -3,43 ± 0,90 | 3,43 ± 0,1 |
| *Hystrix major* (ad.) | VM-93-3B-96 | fragment of incisor tooth | -- | -- | -3,5 | -- |
| *Pachycrocuta brevirostris* (ad.) | VM-2226 | ulna | -22,5 | +6,1 | -4,0 | 3,4 |
| *Pachycrocuta brevirostris* (ad.) | VM-2004 | third proximal diaphysis of radius | -- | -- | -3,9 | -- |
| *Pachycrocuta brevirostris* (ad.) | VM-2276 | right mandible with $M_1$ | -23,0 | +4,7 | -5,2 | 3,5 |
| *Pachycrocuta brevirostris* (juv.) | VM-460 | skull fragment with left $dP^3$ and $dP^4$ | -- | -- | -3,5 | -- |
| *Pachycrocuta brevirostris* (juv.) | VM-84-C3-H5-6 | left mandible with $dP_2$ and $dP_3$ | -21,5 | +5,8 | -2,3 | 3,6 |
| *Pachycrocuta brevirostris* (juv.) | VM-non coded | fragment of maxilla of a juv. individual | -21,5 | +6,7 | -3,7 | 3,0 |
| Mean for *Pachycrocuta* (N = 4/6) | | | -22,12 ± 0,75 | +5,82 ± 0,84 | -3,77 ± 0,93 | 3,37 ± 0,2 |
| *Homotherium latidens* (ad.) | VM-4340 | right distal tibia of an ad. individual | -21,7 | +6,8 | -3,7 | 3,4 |
| *Homotherium latidens* (ad.) | VM-4340b | right distal tibia of an ad. individual | -22,7 | +6,5 | -5,0 | 3,6 |
| *Homotherium latidens* (ad.) | VM-4516 | left humerus of an ad. individual | -23,9 | +5,6 | -4,7 | 3,4 |
| Mean for *Homotherium* (N = 3/3) | | | -22,77 ± 1,10 | +6,30 ± 0,62 | -4,47 ± 0,68 | 3,47 ± 0,1 |
| *Megantereon whitei* (ad.) | VM-3301 | left distal humerus of an ad. individual | -25,2 | +5,8 | -4,2 | 3,5 |
| *Megantereon whitei* (ad.) | VM-4612 | right distal humerus of an ad. individual | -24,4 | +5,1 | -5,0 | 3,4 |
| Mean for *Megantereon* (N = 2/2) | | | -24,80 ± 0,57 | +5,45 ± 0,49 | -4,60 ± 0,57 | 3,45 ± 0,0 |
| *Panthera* cf. *gombaszoegensis* (ad.) | VM-84-C3-F8-42 | fragment of right mandible | -23,3 | +5,0 | -4,3 | 3,0 |
| *Ursus etruscus* (ad.) | VM-1172 | right distal radius | -- | -- | -3,3 | -- |
| *Ursus etruscus* (ad.) | VM-2972 | right tibia of an ad. individual | -23,8 | +6,7 | -0,4 | 3,3 |
| *Ursus etruscus* (ad.) | VM-1903 | left radius of an ad. individual | -21,9 | +7,4 | -1,9 | 3,1 |
| *Ursus etruscus* (ad.) | VM-non coded | skull | -23,6 | +6,0 | -2,0 | 3,3 |
| Mean for *Ursus* (N = 3/4) | | | -23,10 ± 1,04 | +6,70 ± 0,70 | -1,90 ± 1,19 | 3,23 ± 0,1 |
| *Lycaon lycaonoides* (ad.) | VM-2261 | right maxilla with $P_4$-$M_1$ | -22,7 | +6,5 | -4,8 | 3,5 |
| *Lycaon lycaonoides* (ad.) | VM-2263 | skull (splashed and deformed) of an ad. individual | -23,8 | +5,6 | -5,9 | 3,5 |
| *Lycaon lycaonoides* (ad.) | VM-2259 | fragment of right maxilla of an ad. individual, with $M^1$ | -22,9 | +5,2 | -3,7 | 3,4 |
| Mean for *Lycaon* (N = 3/3) | | | -23,13 ± 0,59 | +5,77 ± 0,67 | -4,80 ± 1,10 | 3,47 ± 0,0 |
| *Canis mosbachensis* (ad.) | VM-2254 | left mandible with $M_2$ and roots of $P_3$-$P_4$-$M_1$ | -23,5 | +5,3 | -4,8 | 3,6 |
| *Canis mosbachensis* (ad.) | VM-2254b | left mandible with $M_2$ and roots of $P_3$-$P_4$-$M_1$ | -21,8 | +4,1 | -3,7 | 3,5 |
| *Canis mosbachensis* (subad.) | VM-4440 | right mandible, $M_1$ with non developed roots | -22,2 | +4,7 | -4,6 | 3,3 |
| Mean for *Canis* (N = 3/3) | | | -22,50 ± 0,89 | +4,70 ± 0,60 | -4,37 ± 0,59 | 3,47 ± 0,1 |

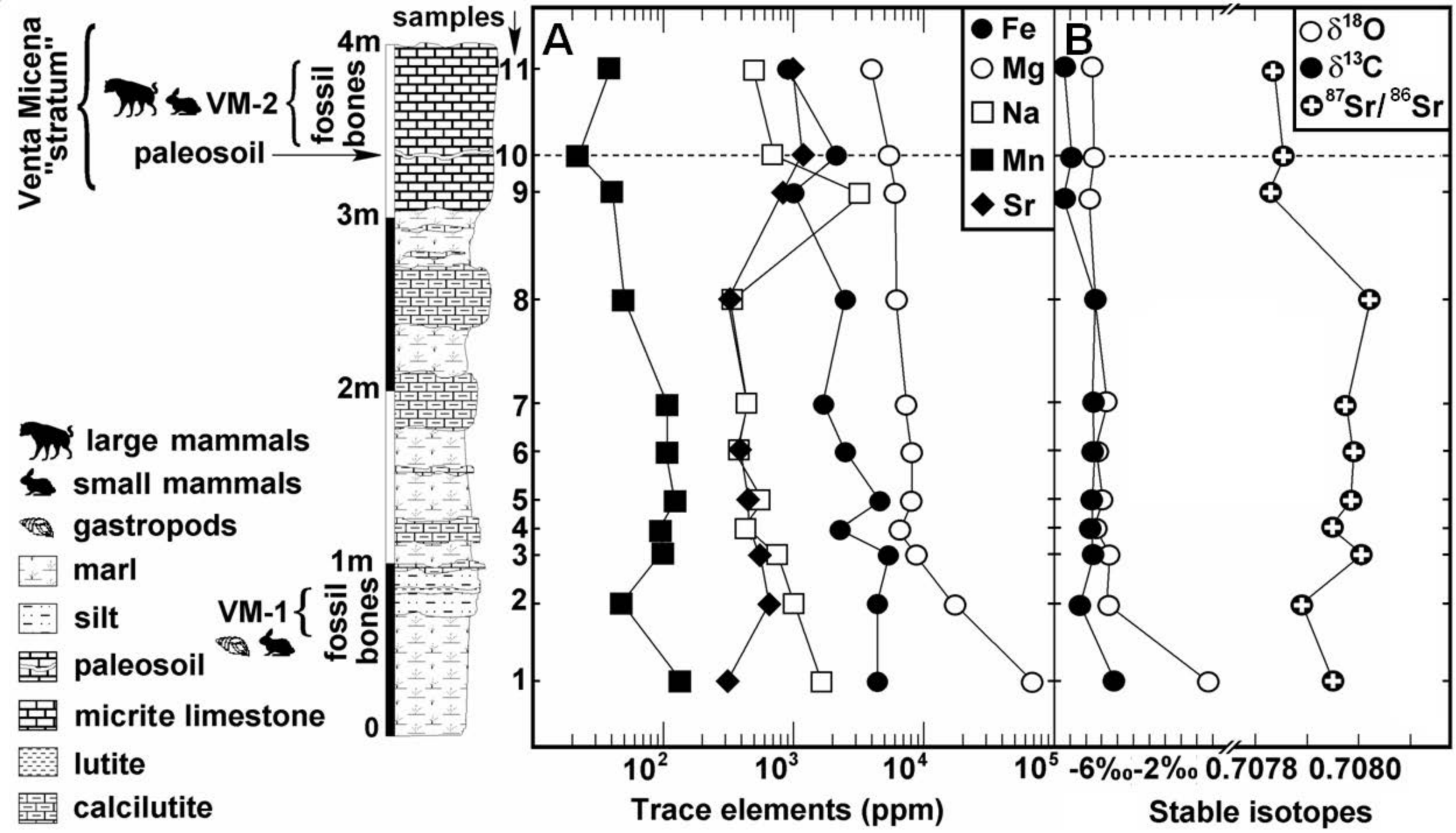
Venta Micena "stratum"
VM-2
fossil bones
paleosoil
4m
3m
2m
1m
0
samples
11
10
9
8
7
6
5
4
3
2
1
VM-1
fossil bones
large mammals
small mammals
gastropods
marl
silt
paleosoil
micrite limestone
lutite
calcilutite
A
Fe
Mg
Na
Mn
Sr
B
δ18O
δ13C
87Sr/86Sr
10^2
10^3
10^4
10^5
Trace elements (ppm)
-6‰
-2‰
0.7078
0.7080
Stable isotopes

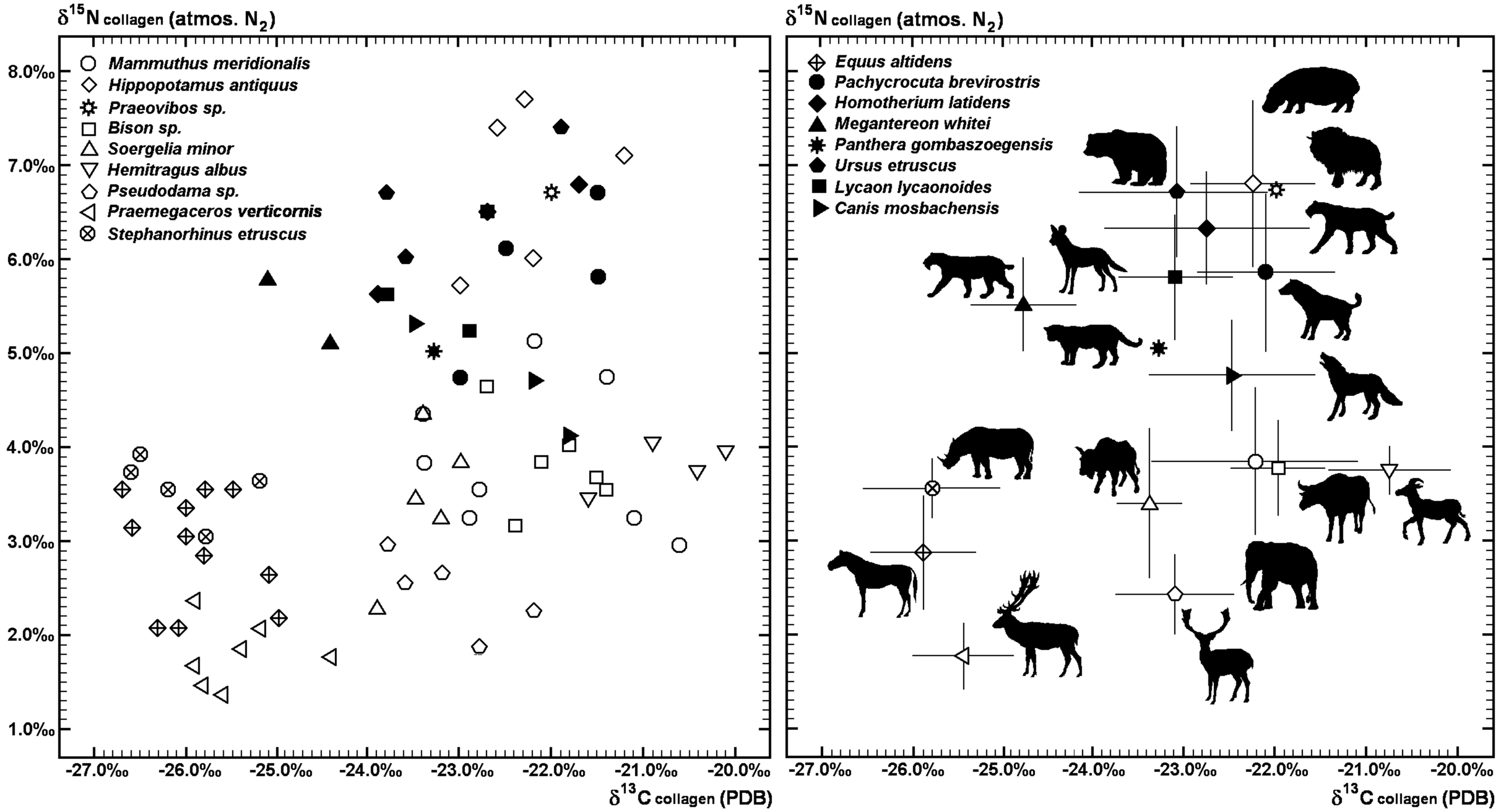
δ15N collagen (atmos. N2)
Mammuthus meridionalis
Hippopotamus antiquus
Praeovibos sp.
Bison sp.
Soergelia minor
Hemitragus albus
Pseudodama sp.
Praemegaceros verticornis
Stephanorhinus etruscus
8.0‰
7.0‰
6.0‰
5.0‰
4.0‰
3.0‰
2.0‰
1.0‰
-27.0‰
-26.0‰
-25.0‰
-24.0‰
-23.0‰
-22.0‰
-21.0‰
-20.0‰
δ13C collagen (PDB)
δ15N collagen (atmos. N2)
Equus altidens
Pachycrocuta brevirostris
Homotherium latidens
Megantereon whitei
Panthera gombaszoegensis
Ursus etruscus
Lycaon lycaonoides
Canis mosbachensis
-27.0‰
-26.0‰
-25.0‰
-24.0‰
-23.0‰
-22.0‰
-21.0‰
-20.0‰
δ13C collagen (PDB)

$\bar{X} - \sigma_x$ $\bar{X} + \sigma_x$

25th perc. 75th perc.

outlier median

perissodactyls (monogastric) and browsing deer (canopy effect)

most foregut fermenters (ruminant artiodactyls) and elephants (monogastric)

$\delta^{13}C_{collagen}$

-27‰ -26‰ -25‰ -24‰ -23‰ -22‰ -21‰ -20‰

closed habitat

open habitat

($N_2$-fixing vegetation)

aquatic plants lichens

$\delta^{15}N_{collagen}$

+1‰ +2‰ +3‰ +4‰ +5‰ +6‰ +7‰ +8‰

Herbivores

(N = 8)

(N = 5)

(N = 6)

(N = 1)

(N = 5)

(N = 4)

(N = 5)

(N = 7)

(N = 6)

(N = 11)

trophic level enrichment

Carnivores

(N = 4)

(N = 3)

(N = 2)

(N = 1)

(N = 3)

(N = 3)

(N = 3)

trophic level enrichment

$\bar{X} - \sigma_x$ $\bar{X} + \sigma_x$

25th perc. 75th perc.

outlier median

increased water dependence

water requirements obtained from vegetation

$\delta^{18}O_{hydroxylapatite}$

-8‰ -6‰ -4‰ -2‰ 0‰

Herbivores

(N = 13)

(N = 7)

(N = 11)

(N = 1)

(N = 5)

(N = 6)

(N = 8)

(N = 12)

(N = 11)

(N = 18)

(N = 1)

trophic level depletion

Carnivores

(N = 6)

(N = 3)

(N = 2)

(N = 1)

(N = 4)

(N = 3)

(N = 3)

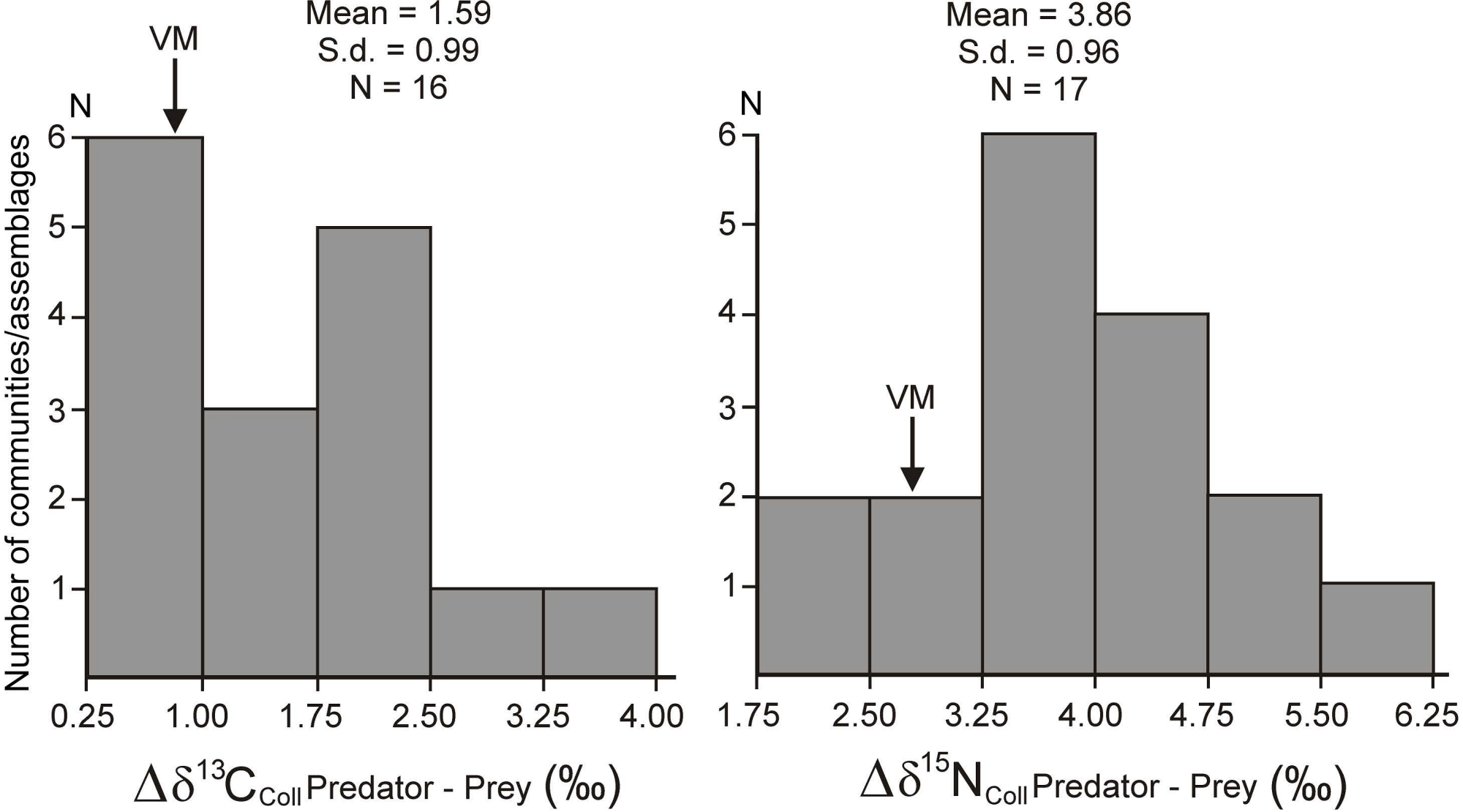
Mean = 1.59
S.d. = 0.99
N = 16
VM
N
Number of communities/assemblages
0.25
1.00
1.75
2.50
3.25
4.00
$\Delta\delta^{13}C_{Coll}$ Predator - Prey (‰)
Mean = 3.86
S.d. = 0.96
N = 17
VM
N
1.75
2.50
3.25
4.00
4.75
5.50
6.25
$\Delta\delta^{15}N_{Coll}$ Predator - Prey (‰)

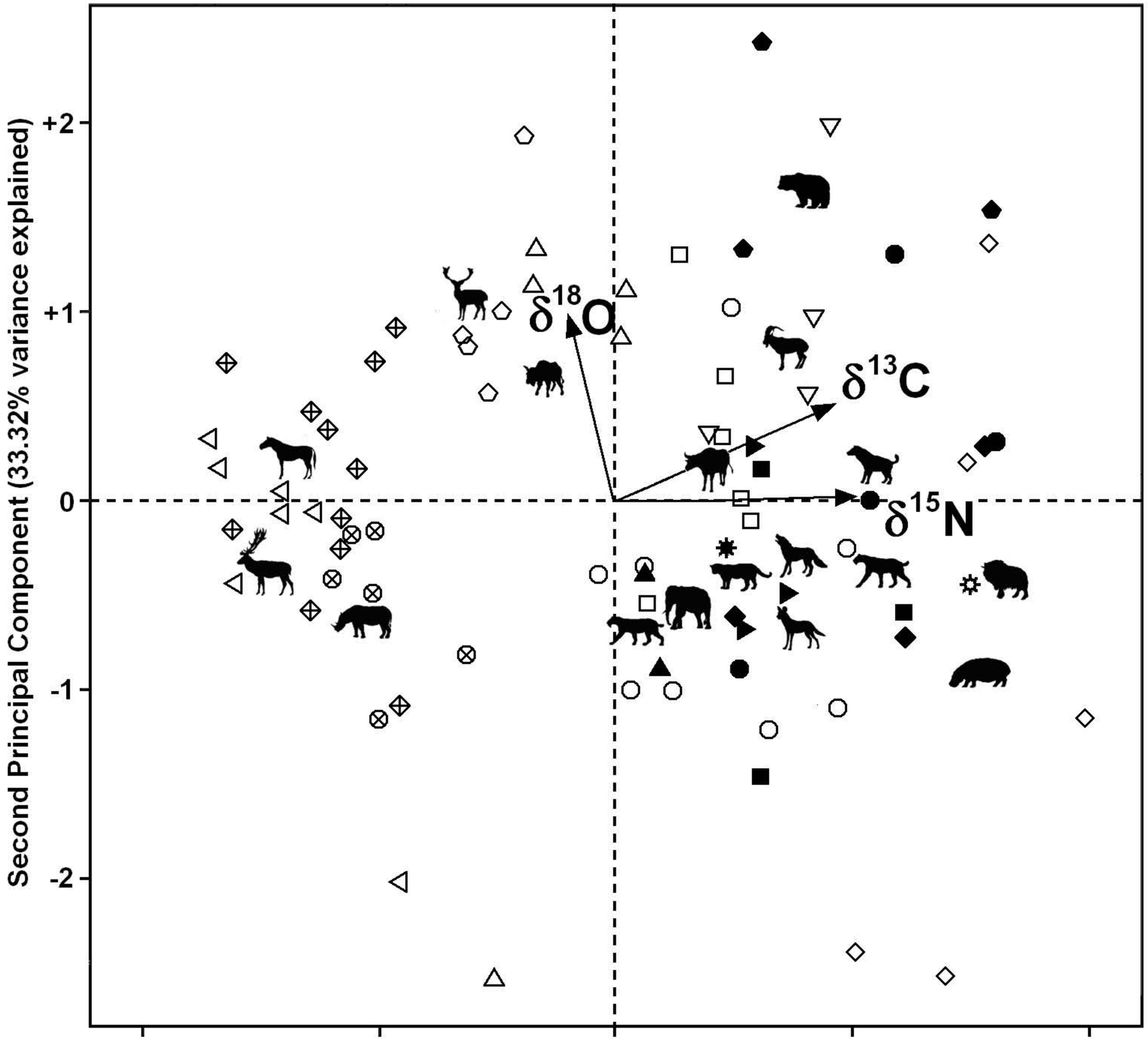
δ18O
δ13C
δ15N
+2
+1
0
-1
-2
-2
-1
0
+1
+2
Second Principal Component (33.32% variance explained)
First Principal Component (48.74% variance explained)

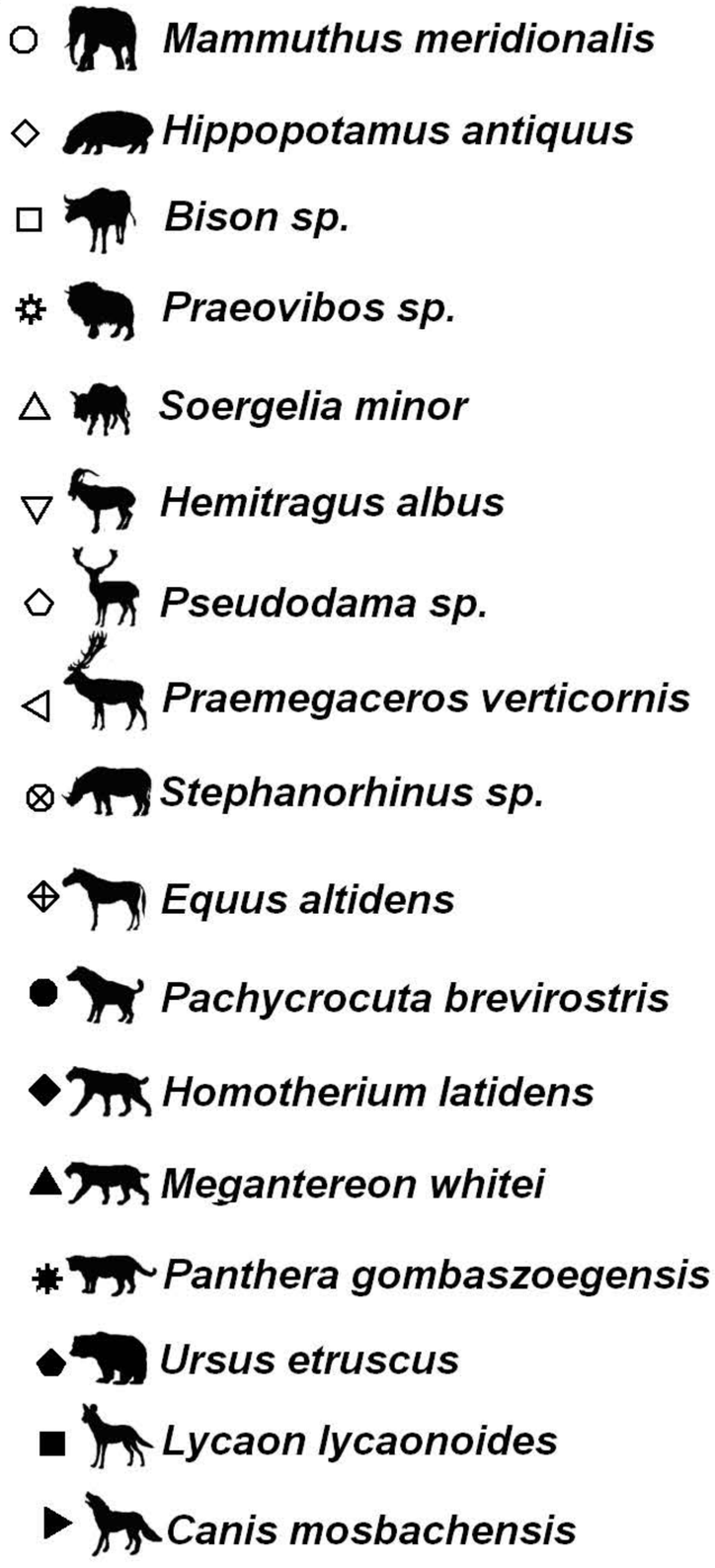
Mammuthus meridionalis
Hippopotamus antiquus
Bison sp.
Praeovibos sp.
Soergelia minor
Hemitragus albus
Pseudodama sp.
Praemegaceros verticornis
Stephanorhinus sp.
Equus altidens
Pachycrocuta brevirostris
Homotherium latidens
Megantereon whitei
Panthera gombaszoegensis
Ursus etruscus
Lycaon lycaonoides
Canis mosbachensis


A


B


C


D

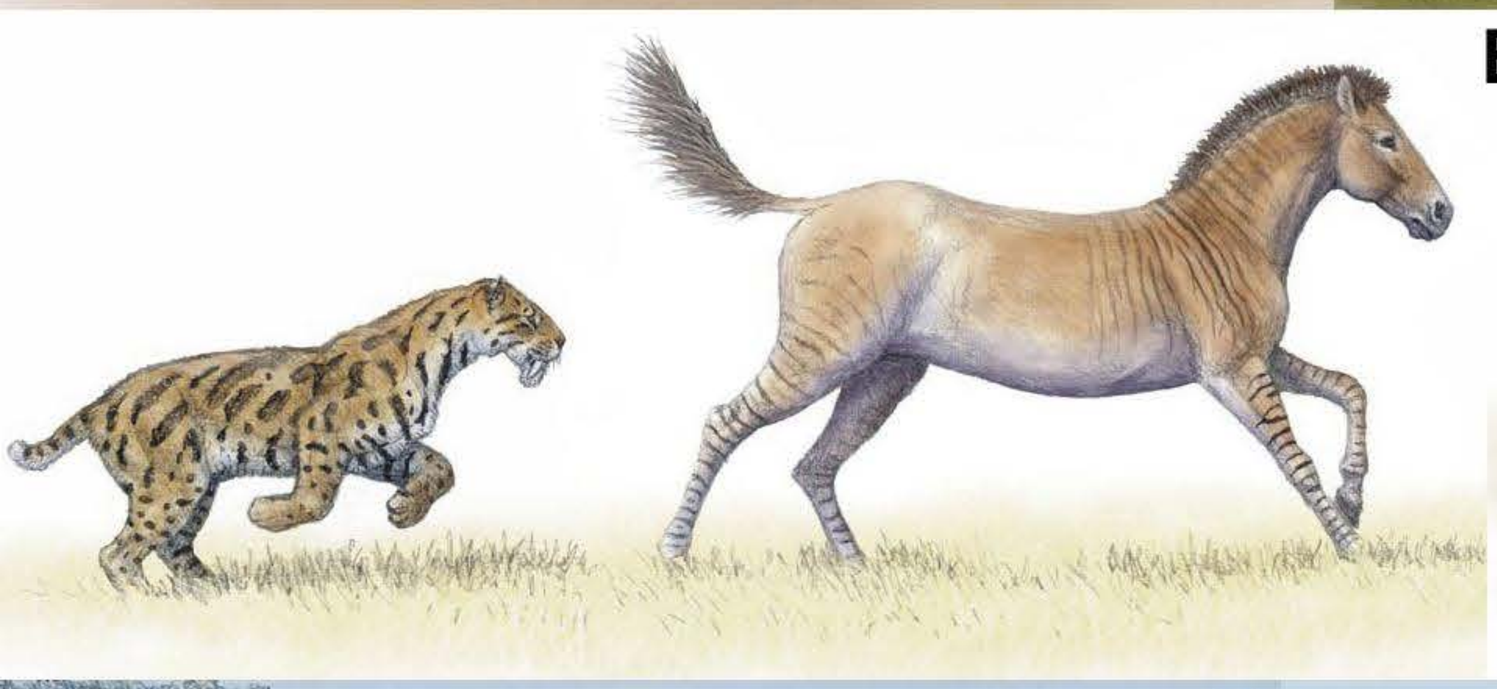
E


F

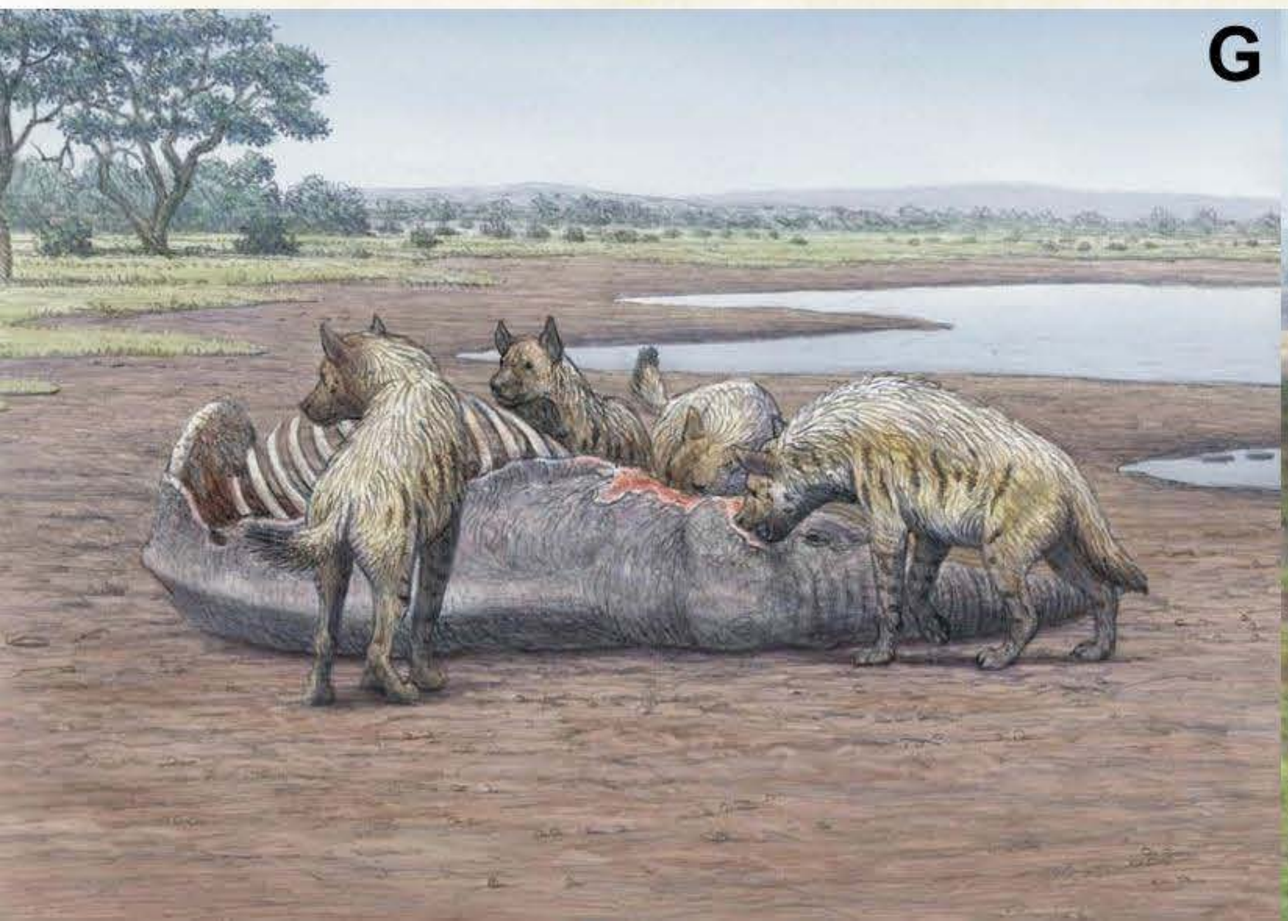
G


H

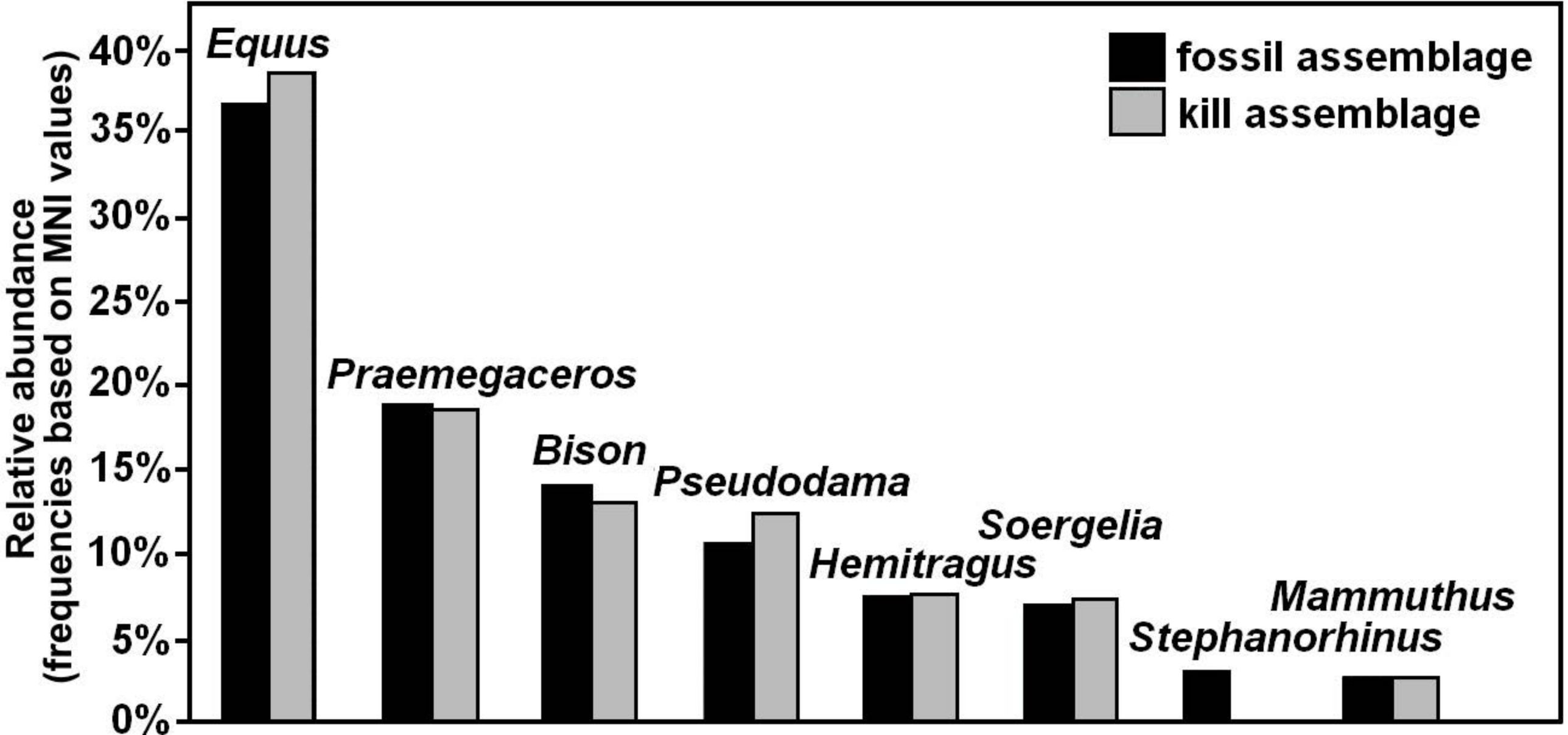
Relative abundance
(frequencies based on MNI values)
40%
35%
30%
25%
20%
15%
10%
5%
0%
Equus
Praemegaceros
Bison
Pseudodama
Hemitragus
Soergelia
Stephanorhinus
Mammuthus
fossil assemblage
kill assemblage